

Re: (nhess-2017-336) Assessment of peak tsunami amplitude associated with a great earthquake occurring along the southernmost Ryukyu subduction zone for Taiwan region by Yu-Sheng Sun, Po-Fei Chen, Chien-Chih Chen, Ya-Ting Lee, Kuo-Fong Ma, and Tso-Ren Wu

Dear Prof. Lionello,

Thank you for reviewing this paper. We have made the revision to our manuscript intensively and reply the comments from reviewers carefully for your further consideration on the publication in Natural Hazards and Earth System Sciences (*NHESS*).

The authors highly appreciate the support of publication in *NHESS* from the reviewers and their helpful suggestion as well. We have made substantive modifications according to their suggestion. We deeply appreciate their suggestion, which has made the manuscript become much better. The annotated responses to the reviewers' comments and the details about our changes in the revised version of our manuscript are made accordingly in the files.

Attached please also find the electronic files of the revised manuscript for your further consideration of publication in *NHESS*. In the revised version, all modifications were marked in red for your reference. Any problem raised please let me know. Thank you very much.

With Best Regards,
Yu-Sheng Sun

Response (in black) to the comments of Reviewer (in blue)

Reviewer #1:

3. Are these up to international standards?
4. Are the scientific methods and assumptions valid and outlined clearly?
7. Is the description of the data used, the methods used, the experiments and calculations made, and the results obtained sufficiently complete and accurate to allow their reproduction by fellow scientists (traceability of results)?

Concerning the application of the tsunami model: No. COMCOT is used as a black box. My major criticism is that the model is not validated for this area, and I strongly suggest to add a hind cast of a real event to prove that COMCOT with the chosen settings delivers realistic simulations. Probably, the last near field tsunami in 1867 is not well suited for a hind cast due to the lack of measurements, but the Tohoku tsunami 2011 should be a good test case also for Taiwan.

We have added some references in text. [Page 6, lines 2-6]

To solve the time dependent tsunami propagation, we adopt a well-validated numerical model, COMCOT (Cornell Multi-grid Coupled Tsunami Model). COMCOT is able to solve both linear and nonlinear shallow water equations on a Cartesian or Spherical coordinate systems (Wang 2009). In terms of validation, COMCOT has been widely used in studying many historical tsunami events, such as 1960 Chilean tsunami (Liu et al., 1995), 1992 Flores Islands tsunami (Liu et al., 1995), 2003 Algeria tsunami (Wang and Liu, 2005), 2004 Indian Ocean tsunami (Wang and Liu, 2006, 2007), and 2006 Ping-Tung tsunami (Wu, et al., 2008; Chen, et al., 2008). Taking the explicit leap-frog scheme to solve shallow water equation, COMCOT has the 2nd order accuracy in both space and time domains. COMCOT also supports the nested grid system that the finer grid can be placed on a coarser grid to increase the resolution locally. Thus, we can use finer grid in near-shore region and coarser grid in deep sea region.

Reference:

- Chen, P. F., Newman, A. V., Wu, T. R., and Lin, C. C. (2008). Earthquake Probabilities and Energy Characteristics of Seismicity Offshore Southwest Taiwan. *Terr. Atmos. Ocean. Sci.*, 6, 697-703, doi: 10.3319/TAO.2008.19.6.697(PT)
- Liu, P. L. F., Cho, Y. S., Yoon, S. B., and Seo, S. N. (1995). Numerical simulations of the 1960 Chilean tsunami propagation and inundation at Hilo, Hawaii. In *Tsunami: Progress in prediction, disaster prevention and warning* (pp. 99-115). Springer,

Dordrecht. https://doi.org/10.1007/978-94-015-8565-1_7

- Liu, P. L. F., Cho, Y. S., Briggs, M. J., Kanoglu, U., and Synolakis, C. E. (1995). Runup of solitary waves on a circular island. *J. Fluid Mech.*, 302, 259-285. doi: 10.1017/S0022112095004095
- Wang, X. (2009). User manual for COMCOT version 1.7 (first draft). Cornell University, 65.
- Wang, X., and Liu, P. L. (2005). A numerical investigation of Boumerdes-Zemmouri (Algeria) earthquake and tsunami. *Comput. Model. Eng. Sci.*, 10(2), 171.
- Wang, X., & Liu, P. L. F. (2006). An analysis of 2004 Sumatra earthquake fault plane mechanisms and Indian Ocean tsunami. *J. Hydraul. Res.*, 44(2), 147-154. doi: 10.1080/00221686.2006.9521671
- Wang, X., & Liu, P. L. F. (2007). Numerical simulations of the 2004 Indian Ocean tsunamis—coastal effects. *Journal of Earthquake and Tsunami*, 1(03), 273-297.
- Wu, T. R., Chen, P. F., Tsai, W. T., & Chen, G. Y. (2008). Numerical study on tsunamis excited by 2006 Pingtung earthquake doublet. *Terr. Atmos. Ocean. Sci.* doi: 10.3319/TAO.2008.19.6.705(PT)

The following questions should be addressed:

Which formulas and parameters are used, in particular for bottom friction (Manning coefficient)? The bottom friction has an impact on the simulated tsunami amplitude at the coast.

We have added the description of Manning coefficient. [Page 6, lines 9-10]

Nonlinear shallow water equation for Cartesian coordinate is used:

$$\frac{\partial \eta}{\partial t} + \frac{\partial P}{\partial x} + \frac{\partial Q}{\partial y} = -\frac{\partial h}{\partial t}$$

$$\frac{\partial P}{\partial t} + \frac{\partial}{\partial x} \left\{ \frac{P^2}{H} \right\} + \frac{\partial}{\partial y} \left\{ \frac{PQ}{H} \right\} + gH \frac{\partial \eta}{\partial x} + F_x = 0$$

$$\frac{\partial Q}{\partial t} + \frac{\partial}{\partial x} \left\{ \frac{PQ}{H} \right\} + \frac{\partial}{\partial y} \left\{ \frac{Q^2}{H} \right\} + gH \frac{\partial \eta}{\partial y} + F_y = 0$$

η is the free-surface displacement. P and Q are the horizontal volume discharges. g is gravity. h is the still water depth. H is the total water depth, $H = \eta + h$. F_x and F_y are the bottom frictions.

$$F_x = \frac{gn^2}{H^{7/3}} P(P^2 + Q^2)^{1/2}$$

$$F_y = \frac{gn^2}{H^{7/3}} Q(P^2 + Q^2)^{1/2}$$

n is Manning's roughness coefficient. In this study, Manning coefficient is 0.013, which

represents a smooth surface (Wu, et al., 2008; Wang 2009).

Reference:

Wang, X. (2009). User manual for COMCOT version 1.7 (first draft). Cornell University, 65.

Wu, T. R., Chen, P. F., Tsai, W. T., and Chen, G. Y.: Numerical Study on Tsunamis Excited by 2006 Pingtung Earthquake Doublet, Terr. Atmos. Ocean. Sci., 19, 705-715, 2008. doi: 10.3319/TAO.2008.19.6.705(PT)

Which bathymetry and topography data is used? Free GEBCO and SRTM?

We have added it. [Page 6, lines 10-11]

The resolution of 1 minute for the inner mesh is quite rough for simulations that should give estimates of the tsunami amplitude at the coast. Our experience from hind casts of real events suggests that at the coast line, the horizontal resolution should be 500m (edge length in an unstructured triangular grid) or better. This should be transferable, as COMCOT also is a model with first order spatial discretization.

The Figure 1 presents the time series by uniform slip distribution at station 25 in different resolution of topography. The time series are similar. For resolution, 1 minute is better than 2 minute and for time spent, 1 minute is less than 30 arc-sec. Therefore, to consider the resolution of simulation and time spent, the resolution of 1 minute was applied.

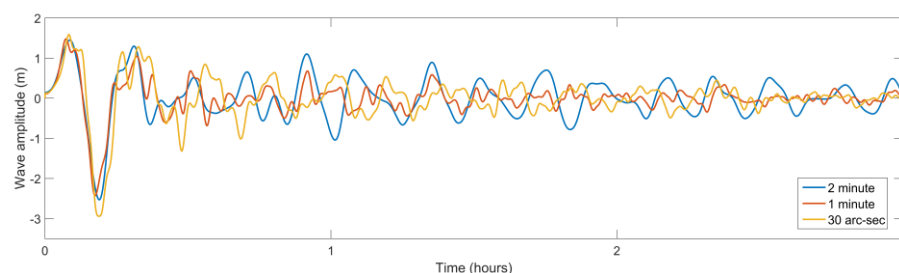


Fig. 1 The time series by uniform slip distribution at station 25 in different resolution of topography. Blue line is 2 minute, red line is 1 minute and yellow line is 30 arc-sec.

Where are the tide gauges located? See also point 14, references. On the one hand, the exact location is not really important, because the study could be performed with virtual sensor locations or coastal forecast points, but

- to reproduce the results, the locations of the (real or virtual) gauges are needed,
- for hind casts of real events, the location and measurements from real tide gauges are needed,

- the simulation of the tsunami wave form at a tide gauge that is located e.g., inside a harbor or narrow bight is very sensitive to errors in the representation of bathymetry and topography (1min resolution for sure is too coarse!) and to the choice of the roughness parameter (wave reflections).
- The comparison in fig. 6 may be spoiled by different gauge locations. Distance to the source is not the only parameter, as it is also stated in the paper, too (e.g., page 7 line 23-24).

We have added location information and removed fitting line [Page 6, lines 13-18; Pages 20-21]

We list the location of the gauges in the Table 1.

Table 1. The tide gauge locations in this study.

No.	Station	Lon	Lat
1	Linshanbi	121.5106	25.2844
2	Danshuei	121.4019	25.1844
3	Jhuwei	121.2353	25.1200
4	Hsinchu	120.9122	24.8503
5	Waipu	120.7717	24.6514
6	Taichung Port	120.5250	24.2917
7	Fanyuan	120.2972	23.9147
8	Bozihliao	120.1417	23.6250
9	Penghu	119.5669	23.5636
10	Dongshih	120.1417	23.4417
11	Jiangyun	120.1000	23.2181
12	Anping	120.1583	22.9750
13	Yongan	120.1917	22.8083
14	Kaohsiung	120.2883	22.6144
15	Donggang	120.4417	22.4583
16	Siaoliouciou	120.3750	22.3583
17	Jiahe	120.6083	22.3250
18	Syunguangzuei	120.6917	21.9917
19	Houbihu	120.7583	21.9417
20	Lanyu	121.4917	22.0583
21	Dawu	120.8972	22.3375
22	Lyudao	121.4647	22.6622
23	Fugang	121.1917	22.7917

24	Chenggong	121.3767	23.0889
25	Shihti	121.5250	23.4917
26	Hualien	121.6231	23.9803
27	Suao	121.8686	24.5856
28	Gengfang	121.8619	24.9072
29	Longdong	121.9417	25.1250
30	Keelung	121.7417	25.1750

The fittings of Fig. 6 just give a rough relationship between wave height and distance for the tsunami source which is perpendicular the coast line. Of course, the distance is not the only parameter for wave height attenuation. We agree to remove the fitting lines.

11. Are mathematical formulae, symbols, abbreviations and units correctly defined and used? If the formulae, symbols or abbreviations are numerous, are there tables or appendixes listing them?

Equation (1): W for width, L for length: It's obvious, but nevertheless should be added in the text above. Which value for μ is assumed when estimating M_w ? And as a non-seismologist, I would like to ask if the estimate of $D = 8.25\text{m}$ is really obvious? Section 2.2: Not my field of expertise at all.

We have done it. [Page 3, lines 21-23]

We will add the definition of symbols (W and L) in the text. μ usually sets 30GPa and it assumes that crust is elastically uniform. The estimation of slip and M_w is from fault geometry and parameter assuming as μ .

We analyzed the relation between M_w and average slip (D) in Fig 2. The public finite fault slip models of global slip earthquakes are from the website (<http://quake-rc.info/SRCMOD/>). This figure appears the trend between M_w and average slip and its boundary. For $M_w 8.15$, the range could be 200~1000 cm. It explains that our estimation, which follows the trend and in the possible boundary, is reasonable.

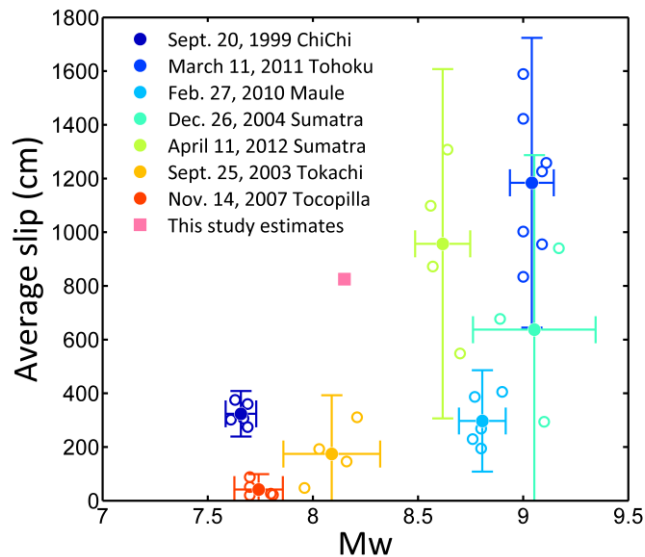


Fig 2. Mw of real events and their average slips with 2 standard deviation (<http://equake-rc.info/SRCMOD/>). Open circles represent the inverse slip results in each study. Solid circles represent the mean slip of each study for same event.

ChiChi (1999): Ma et al. (2000); Chi et al. (2001); Zeng and Chen (2001); Wu et al. (2001); Zhang et al. (2004)

Tohoku (2011): Ammon et al. (2011); Ide et al. (2011); Lay et al. (2011); Shao et al. (2011); Yagi and Fukahata (2011); Yamazaki et al. (2011); Wei et al. (2012)

Maule (2010): Delouis et al. (2010); Hayes (2010); Shao et al. (2010); Sladen (2010); Luttrell et al. (2011)

Sumatra (2004): Ammon et al. (2005); Ji (2005); Rhie et al. (2007)

Sumatra (2012): Hayes (2012); Shao et al. (2012); Wei (2012); Yue et al. (2012)

Tokachi-Oki (2003): Yamanaka and Kikuchi (2003); Koketsu et al. (2004); Tanioka et al. (2004); Yagi (2004)

Tocopilla (2007): Ji (2007); Sladen (2007); Zeng et al. (2007); Béjar-Pizarro et al. (2010); Motagh et al. (2010)

Reference:

Ammon, C. J., J. Chen, H.-K. Thio, D. Robinson, S. Ni, V. Hjorleifsdottir, H. Kanamori, T. Lay, S. Das, D. Helmberger, G. Ichinose, J. Polet, and D. Wald. (2005). Rupture process of the great 2004 Sumatra-Andaman earthquake, *Science*, 308, 1133-1139.

Ammon, C. J., T. Lay, H. Kanamori, and M. Cleveland (2011) A rupture model of the 2011 off the Pacific coast of Tohoku Earthquake, *Earth Planets Space*, 63, 693–696.

Bejar-Pizarro M., Carrizo D., Socquet A., Armijo R., (2010) Asperities, barriers and

- transition zone in the North Chile seismic gap: State of the art after the 2007 Mw 7.7 Tocopilla earthquake inferred by GPS and InSAR data, *Geoph. Journ. Int.*, GJI-S-09-0648, doi: 10.1111/j.1365-246X.2010.04748.x
- Chi, W. C., D. Dreger, and A. Kaverina. 2001. Finite-source modeling of the 1999 Taiwan (Chi-Chi) earthquake derived from a dense strong-motion network. *Bull. Seis. Soc. Am* 91 (5):1144-1157.
- Delouis B., J. M. Nocquet, M. Vallée (2010). Slip distribution of the February 27, 2010 Mw = 8.8 Maule Earthquake, central Chile, from static and high-rate GPS, InSAR, and broadband teleseismic data, *Geophys. Res. Lett.*, 37, L17305, doi:10.1029/2010GL043899.
- Hayes G., (NEIC, Maule 2010) Updated Result of the Feb 27, 2010 Mw 8.8 Maule, Chile Earthquake, http://earthquake.usgs.gov/earthquakes/eqinthenews/2010/us2010tfan/finite_fault.php, last accessed August 19, 2013.
- Hayes G., (NEIC, Sumatra 2012) Preliminary Result of the Apr 11, 2012 Mw 8.6 Earthquake Off the West Coast of Northern Sumatra, http://earthquake.usgs.gov/earthquakes/eqinthenews/2012/usc000905e/finite_fault.php, last accessed August 19, 2013.
- Ide S., A. Baltay, and G. C. Beroza (2011). Shallow Dynamic Overshoot and Energetic Deep Rupture in the 2011 Mw 9.0 Tohoku-Oki Earthquake, 332, 1426-1429, DOI: 10.1126/science.1207020
- Ji, C. (2005). Preliminary Rupture Model for the December 26, 2004 earthquake, off the west coast of northern Sumatra, magnitude 9.1, http://neic.usgs.gov/neis/eq_depot/2004/eq_041226/neic_slav_ff.html.
- Ji C. (UCSB, Tocopilla 2007) Preliminary Result of the Nov 14, 2007 Mw 7.81 ANTOFAGASTA, CHILE Earthquake, http://www.geol.ucsb.edu/faculty/ji/big_earthquakes/2007/11/anto/anto.html, last accessed August 11, 2013.
- Koketsu, K., K. Hikima, S. Miyazaki, and S. Ide. (2004). Joint inversion of strong motion and geodetic data for the source process of the 2003 Tokachi-oki, Hokkaido, earthquake. *Earth Planets and Space* 56 (3):329-334.
- Lay T., C. J. Ammon, H. Kanamori, L. Xue, and M. J. Kim (2011). Possible large near-trench slip during the 2011 Mw 9.0 off the Pacific coast of Tohoku Earthquake. *Earth Planets Space*. 63, 687–692.
- Luttrell, K. M., Tong, X., Sandwell, D. T., Brooks, B. A., and Bevis, M. G. (2011). Estimates of stress drop and crustal tectonic stress from the 27 February 2010 Maule, Chile, earthquake: Implications for fault strength. *Journal of Geophysical Research: Solid Earth* (1978–2012), 116(B11).

- Ma, K. F., T. R. A. Song, S. J. Lee, and H. I. Wu. (2000). Spatial slip distribution of the September 20, 1999, Chi-Chi, Taiwan, earthquake (M(W)7.6) - Inverted from teleseismic data. *Geophys. Res. Lett.* 27 (20):3417-3420.
- Motag, M., B. Schurr, J. Anderssohn, B. Cailleau, T. R. Walter, R. Wang, J.-P. Villotte, (2010) Subduction earthquake deformation associated with 14 November 2007, Mw 7.8 Tocopilla earthquake in Chile: Results from InSAR and aftershocks, *Tectonophysics* 490, 60–68
- Rhie, J., D. Dreger, R. Burgmann, and B. Romanowicz. (2007). Slip of the 2004 Sumatra–Andaman Earthquake from joint inversion of long-period global seismic waveforms and GPS static Offsets, *Bull. Seismo. Soc. Am.*, 97(1A): S115–S127.
- Shao, G., X. Li and C. Ji. (UCSB, sumatra 2012). Preliminary Result of the Apr 11, 2012 Mw 8.64 sumatra Earthquake, http://www.geol.ucsb.edu/faculty/ji/big_earthquakes/2012/04/10/sumatra.html, last accessed August 19, 2013.
- Shao, G., X. Li, C. Ji. and T. Maeda (2011). Focal mechanism and slip history of 2011 Mw 9.1 off the Pacific coast of Tohoku earthquake, constrained with teleseismic body and surface waves, *Earth Planets Space*, 63 (7), 559-564.
- Shao, G., X. Li, Q. Liu, X. Zhao, T. Yano and C. Ji(UCSB, Maule 2010). Preliminary slip model of the Feb 27, 2010 Mw 8.9 Maule, Chile Earthquake, http://www.geol.ucsb.edu/faculty/ji/big_earthquakes/2010/02/27/chile_2_27.html, last accessed September 24, 2013.
- Sladen A. (Caltech, Tocopilla 2007). Preliminary Result 11/14/2007 (Mw 7.7), Tocopilla Earthquake, Chile. Source Models of Large Earthquakes. http://www.tectonics.caltech.edu/slip_history/2007_tocopilla/tocopilla.html, last accessed July 1, 2013.
- Sladen A. (Caltech, Maule 2010). Preliminary Result, 02/27/2010 (Mw 8.8), Chile. Source Models of Large Earthquakes. http://www.tectonics.caltech.edu/slip_history/2010_chile/index.html.
- Tanioka, Y., K. Hirata, R. Hino, and T. Kanazawa. (2004). Slip distribution of the 2003 Tokachi-oki earthquake estimated from tsunami waveform inversion. *Earth Planets and Space* 56 (3):373-376.
- Wei S. (Caltech, Sumatra 2012). April/11/2012 (Mw 8.6), Sumatra. Source Models of Large Earthquakes. http://www.tectonics.caltech.edu/slip_history/2012_Sumatra/index.html, last accessed July 1, 2013.
- Wei, S. J., R.W. Graves, D. Helmberger, J.P. Avouac and J.L. Jiang (2012) Sources of shaking and flooding during the Tohoku-Oki earthquake: A mixture of rupture styles, *Earth and Planetary Science Letters*, 333-334, 91-100.

- Wu, C. J., M. Takeo, and S. Ide. (2001). Source process of the Chi-Chi earthquake: A joint inversion of strong motion data and global positioning system data with a multifault model. *Bull. Seis. Soc. Am* 91 (5):1128-1143.
- Yagi, Y. (2004). Source rupture process of the 2003 Tokachi-oki earthquake determined by joint inversion of teleseismic body wave and strong ground motion data, *Earth Planets Space*, 56, 311–316.
- Yagi, Y. and Fukahata, Y., (2011). Rupture process of the 2011 Tohoku-oki earthquake and absolute elastic strain release, *Geophys. Res. Lett.*, 38, L19307, doi:10.1029/2011GL048701.
- Yamanaka, Y., and M. Kikuchi. (2003). Source process of the recurrent Tokachi-oki earthquake on September 26, 2003, inferred from teleseismic body waves. *Earth Planets and Space* 55 (12):E21-E24.
- Yamazaki, Y., T. Lay, K. F. Cheung, H. Yue, and H. Kanamori (2011). Modeling near-field tsunami observations to improve finite-fault slip models for the 11 March 2011 Tohoku earthquake, *Geophys. Res. Lett.*, 38, L00G15, doi:10.1029/2011GL049130.
- Yue, H, T. Lay and K. D. Koper (2012), En Echelon and Orthogonal Fault Ruptures of the 11 April 2012 Great Intraplate Earthquakes. *Nature*, 490, 245-249, doi:10.1038/nature11492.
- Zeng, Y. H., and C. H. Chen. (2001). Fault rupture process of the 20 September 1999 Chi-Chi, Taiwan, earthquake. *Bull. Seis. Soc. Am* 91 (5):1088-1098.
- Zeng, Y., G. Hayes and C. Ji (2007; USGS, Online Model). Preliminary Result of the Nov 14, 2007 Mw 7.7 Antofagasto, Chile Earthquake, http://earthquake.usgs.gov/earthquakes/eqinthenews/2007/us2007jsat/finite_fault.php, last accessed August 20, 2013.
- Zhang, W., T. Iwata, K. Irikura, A. Pitarka, and H. Sekiguchi (2004), Dynamic rupture process of the 1999 Chi-Chi, Taiwan, earthquake, *Geophys. Res. Lett.*, 31, L10605, doi:10.1029/2004GL019827.

12. Is the size, quality and readability of each figure adequate to the type and quantity of data presented?

Figure 4: change y-axis label to "Wave amplitude"

Figure 6: I would keep this figure, but skip the explicit linear fitting. It pretends an accuracy that cannot be obtained.

We have done it. [Pages 18, 20]

14. Are the number and quality of the references appropriate?

A citation for the tide gauge locations or at least a list of coordinates would be handy. The Taiwanese tide gauges are not available at <http://www.ioc-sealevelmonitoring.org> or <http://www.psmsl.org/> (Taipei until 1995, Kaohsiung until 1996), and I could not find a link to the gauges at the website of the Taiwanese Central Weather Bureau (CWB) <http://www.cwb.gov.tw> This private/commercial site was the best information I could find: <https://www.tide-forecast.com/locations/Hualien-City> . Still, no exact location, but the "Detailed Map" gives at least an idea that this station is located inside the harbour. In total, 9 Taiwanese stations are available here. I am missing a short overview of historical tsunamis in Taiwan, but the last local tsunami occurred in 1867, and it might be difficult to find scientific papers to cite, see e.g., <http://scweb.cwb.gov.tw/NewsContent.aspx?ItemId=37&CId=199&loc=en> However, I found the following paper - no tsunami, but a report on the uplift of the tide gauge due to the earthquake. Maybe, this paper provides a helpful hindcast, too: COMCOT should not show a strong tsunami. Chung-Liang Lo, Emmy Tsui-Yu Chang, and Benjamin Fong Chao. Relocating the historical 1951 Hualien earthquake in eastern Taiwan based on tide gauge record. *Geophys. J. Int.* (2013) 192, 854–860. doi: 10.1093/gji/ggs058

We have added the information of location. [Page 6, lines 13-18]

The website of Taiwanese Central Weather Bureau (CWB) presents the location of tide stations (<http://e-service.cwb.gov.tw/HistoryDataQuery/index.jsp> and http://www.cwb.gov.tw/V7e/climate/marine_stat/tide.htm).

Lo et al., (2013) investigated the historical 1951 Hualien earthquake sequence. The magnitude of three earthquakes are smaller than our scenario estimation and the focal mechanisms are different from our fault model so that it is not applicable to be compared with our study. This maybe be considered another tsunami earthquake.

15. Are the references accessible by fellow scientists?

Yes, but please add doi numbers.

We have done it. [Pages 11-15]

Reviewer #2:

Page 2, lines 3-5. If the earthquakes associated to the historic tsunamis mentioned in the text have any magnitude estimation, please provide the value and include the reference. For instance, the 1867 tsunami, magnitude?

We have done it. [Page 2, lines 3-4]

The 1867 Keelung earthquake was inferred approximately Mw 7.0 (Tsai 1985; Ma and Lee 1997; Cheng et al., 2016; Yu et al., 2016).

Reference:

Cheng, S. N., Shaw, C. F., and Yeh, Y. T. (2016). Reconstructing the 1867 Keelung Earthquake and Tsunami Based on Historical Documents. *Terr. Atmos. Ocean. Sci.*, 27(3). doi: 10.3319/TAO.2016.03.18.01(TEM)

Ma, K. F., and Lee, M. F. (1997). Simulation of historical tsunamis in the Taiwan region. *Terr. Atmos. Ocean. Sci.*, 8(1), 13-30. doi: 10.3319/TAO.1997.8.1.13(T)

Tsai, Y. B. (1985). A study of disastrous earthquakes in Taiwan, 1683–1895. *Bull. Inst. Earth Sci. Acad. Sin.*, 5, 1-44.

Yu, N.-T., Yen, J.-Y., Chen, W.-S., Yen, I. C., and Liu, J.-H.: Geological records of western Pacific tsunamis in northern Taiwan: AD 1867 and earlier event deposits, *Mar. Geol.*, 372, 1-16, 2016. doi:10.1016/j.margeo.2015.11.010

Page 2, lines 13-15. When comparing PTHA and PSHA, authors mentioned in the text that PSHA works with ground-motion parameters. So, can you complete the idea by specifying that PTHA works with tsunami wave amplitudes, or some other wave measurements? If there is any reference, please include it.

We have done it. [Page 2, lines 14-19]

Geist and Parsons (2006) mentions that the tsunami wave amplitudes follow a definable frequency-size distribution over a sufficiently long amount of time at a given coastal region (Soloviev, 1969; Houston et al., 1977; Horikawa and Shuto, 1983; Burroughs and Tebbens, 2005). This method is of great use in establishing tsunami probability for regions if there is an extensive catalog of observed tsunami wave heights (Geist and Parsons, 2006). The other approach is numerical simulation (Geist, 2002; Geist and Parsons, 2006; Geist and Parsons, 2009) which applies the stochastic slip model to estimate the tsunami amplitudes probability as this study.

Reference:

Burroughs, S.M., Tebbens, S.F. (2005). Power law scaling and probabilistic forecasting of tsunami runup heights. *Pure Appl. Geophys.* 162, 331–342

- Geist, E.L., (2002). Complex earthquake rupture and local tsunamis. *J. Geophys. Res.* 107. doi:10.1029/2000JB000139.
- Geist, E. L., and Parsons, T. (2006). Probabilistic analysis of tsunami hazards. *Natural Hazards*, 37(3), 277-314. doi 10.1007/s11069-005-4646-z
- Geist, E. L., and Parsons, T. (2009). Assessment of source probabilities for potential tsunamis affecting the US Atlantic coast. *Marine Geology*, 264(1), 98-108.
- Horikawa, K. and Shuto, N. (1983). Tsunami disasters and protection measures in Japan, In: K. Iida and T. Iwasaki (eds), *Tsunamis-Their Science and Engineering*, Terra Scientific Publishing Company, pp. 9–22.
- Houston, J. R., Carver, R. D. and Markle, D. G. (1977). Tsunami-wave elevation frequency of occurrence for the Hawaiian Islands. Technical Report H-77-16, U.S. Army Engineer Waterways Experiment Station, Vicksburg, MS, 66 pp.
- Soloviev, S. L. (1969). Recurrence of tsunamis in the Pacific. In: W. M. Adams (ed.), *Tsunamis in the Pacific Ocean*, East-West Center Press, pp. 149–163.

Page 3. Line 2. Please, provide the reference for the magnitude range, Mw 7.5-8.7.

We have done it. [Page 3, line 5]

Reference:

- Hsu, Y. J., Ando, M., Yu, S. B., and Simons, M. (2012). The potential for a great earthquake along the southernmost Ryukyu subduction zone. *Geophysical Research Letters*, 39(14).

Page 3. Line 12. About the fault geometry setting. Which is the source depth of the top (or bottom) of the fault plane? I think it has not been specified yet in the text.

We have done it. [Page 3, lines 14-15]

The fault geometry setting refers to Hsu et al. (2012) and fault model extends from the Ryukyu Trench to a depth of 13 km.

Page 3. Line 15, please complete to "...in dip slip faults".

Thank you. We have done it. [Page 3, line 18]

Page 3. Eq. (1), please, specify what is L, and W.

We have done it. [Page 3, line 21]

Page 3. Line 18. I suggest to change "constant" by "parameter". Strictly speaking, in elastic heterogeneous media, the Lamè parameters (λ and μ) vary in space.

We have done it. [Page 3, line 22]

Page 3. In Eq. (2). Which is the value assumed for μ ?

We have done it. [Page 3, lines 22-23]

Page 3. Section 2.1. When the authors compute the earthquake magnitude, average slip and fault area. Did the authors compare (or contrast) these values with any magnitude/fault-size scaling relationship for subduction earthquakes? It could be interesting to compare these values with any magnitude/size scaling relationship for subduction zones.

We analyzed the relation between M_w and average slip (D) in Fig 1. The public finite fault slip models of global slip earthquakes are from the website (<http://equake-rc.info/SRCMOD/>). This figure appears the trend between M_w and average slip and its boundary. For $M_w 8.15$, the range could be 200~1000 cm. It explains that our estimation, which follows the trend and in the possible boundary, is reasonable.

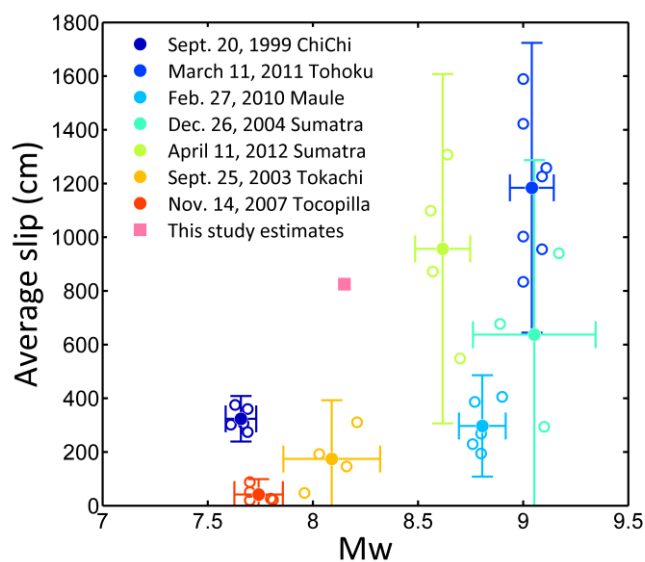


Fig 1. M_w of real events and their average slips with 2 standard deviation (<http://equake-rc.info/SRCMOD/>). Open circles represent the inverse slip results in each study. Solid circles represent the mean slip of each study for same event.

ChiChi (1999): Ma et al. (2000); Chi et al. (2001); Zeng and Chen (2001); Wu et al. (2001); Zhang et al. (2004)

Tohoku (2011): Ammon et al. (2011); Ide et al. (2011); Lay et al. (2011); Shao et al. (2011); Yagi and Fukahata (2011); Yamazaki et al. (2011); Wei et al. (2012)

Maule (2010): Delouis et al. (2010); Hayes (2010); Shao et al. (2010); Sladen (2010); Luttrell et al. (2011)

Sumatra (2004): Ammon et al. (2005); Ji (2005); Rhie et al. (2007)

Sumatra (2012): Hayes (2012); Shao et al. (2012); Wei (2012); Yue et al. (2012)
Tokachi-Oki (2003): Yamanaka and Kikuchi (2003); Koketsu et al. (2004); Tanioka et al. (2004); Yagi (2004)
Tocopilla (2007): Ji (2007); Sladen (2007); Zeng et al. (2007); Béjar-Pizarro et al. (2010); Motagh et al. (2010)

Reference:

- Ammon, C. J., J. Chen, H.-K. Thio, D. Robinson, S. Ni, V. Hjorleifsdottir, H. Kanamori, T. Lay, S. Das, D. Helmberger, G. Ichinose, J. Polet, and D. Wald. (2005). Rupture process of the great 2004 Sumatra-Andaman earthquake, *Science*, 308, 1133-1139.
- Ammon, C. J., T. Lay, H. Kanamori, and M. Cleveland (2011) A rupture model of the 2011 off the Pacific coast of Tohoku Earthquake, *Earth Planets Space*, 63, 693–696.
- Bejar-Pizarro M., Carrizo D., Socquet A., Armijo R., (2010) Asperities, barriers and transition zone in the North Chile seismic gap: State of the art after the 2007 Mw 7.7 Tocopilla earthquake inferred by GPS and InSAR data, *Geoph. Journ. Int.*, GJI-S-09-0648, doi: 10.1111/j.1365-246X.2010.04748.x
- Chi, W. C., D. Dreger, and A. Kaverina. 2001. Finite-source modeling of the 1999 Taiwan (Chi-Chi) earthquake derived from a dense strong-motion network. *Bull. Seis. Soc. Am* 91 (5):1144-1157.
- Delouis B., J. M. Nocquet, M. Vallée (2010). Slip distribution of the February 27, 2010 Mw = 8.8 Maule Earthquake, central Chile, from static and high-rate GPS, InSAR, and broadband teleseismic data, *Geophys. Res. Lett.*, 37, L17305, doi:10.1029/2010GL043899.
- Hayes G., (NEIC, Maule 2010) Updated Result of the Feb 27, 2010 Mw 8.8 Maule, Chile Earthquake, http://earthquake.usgs.gov/earthquakes/eqinthenews/2010/us2010tfan/finite_fault.php, last accessed August 19, 2013.
- Hayes G., (NEIC, Sumatra 2012) Preliminary Result of the Apr 11, 2012 Mw 8.6 Earthquake Off the West Coast of Northern Sumatra, http://earthquake.usgs.gov/earthquakes/eqinthenews/2012/usc000905e/finite_fault.php, last accessed August 19, 2013.
- Ide S., A. Baltay, and G. C. Beroza (2011). Shallow Dynamic Overshoot and Energetic Deep Rupture in the 2011 Mw 9.0 Tohoku-Oki Earthquake, 332, 1426-1429, DOI: 10.1126/science.1207020
- Ji, C. (2005). Preliminary Rupture Model for the December 26, 2004 earthquake, off the west coast of northern Sumatra, magnitude 9.1, http://neic.usgs.gov/neis/eq_depot/2004/eq_041226/neic_slav_ff.html.

- Ji C. (UCSB, Tocopilla 2007) Preliminary Result of the Nov 14, 2007 Mw 7.81 ANTOFAGASTA, CHILE Earthquake, http://www.geol.ucsb.edu/faculty/ji/big_earthquakes/2007/11/anto/anto.html, last accessed August 11, 2013.
- Koketsu, K., K. Hikima, S. Miyazaki, and S. Ide. (2004). Joint inversion of strong motion and geodetic data for the source process of the 2003 Tokachi-oki, Hokkaido, earthquake. *Earth Planets and Space* 56 (3):329-334.
- Lay T., C. J. Ammon, H. Kanamori, L. Xue, and M. J. Kim (2011). Possible large near-trench slip during the 2011 Mw 9.0 off the Pacific coast of Tohoku Earthquake. *Earth Planets Space*. 63, 687–692.
- Luttrell, K. M., Tong, X., Sandwell, D. T., Brooks, B. A., and Bevis, M. G. (2011). Estimates of stress drop and crustal tectonic stress from the 27 February 2010 Maule, Chile, earthquake: Implications for fault strength. *Journal of Geophysical Research: Solid Earth* (1978–2012), 116(B11).
- Ma, K. F., T. R. A. Song, S. J. Lee, and H. I. Wu. (2000). Spatial slip distribution of the September 20, 1999, Chi-Chi, Taiwan, earthquake (M(W)7.6) - Inverted from teleseismic data. *Geophys. Res. Lett.* 27 (20):3417-3420.
- Motag, M., B. Schurr, J. Anderssohn, B. Cailleau, T. R. Walter, R. Wang, J.-P. Villotte, (2010) Subduction earthquake deformation associated with 14 November 2007, Mw 7.8 Tocopilla earthquake in Chile: Results from InSAR and aftershocks, *Tectonophysics* 490, 60–68
- Rhie, J., D. Dreger, R. Burgmann, and B. Romanowicz. (2007). Slip of the 2004 Sumatra–Andaman Earthquake from joint inversion of long-period global seismic waveforms and GPS static Offsets, *Bull. Seismo. Soc. Am.*, 97(1A): S115–S127.
- Shao, G., X. Li and C. Ji. (UCSB, sumatra 2012). Preliminary Result of the Apr 11, 2012 Mw 8.64 sumatra Earthquake, http://www.geol.ucsb.edu/faculty/ji/big_earthquakes/2012/04/10/sumatra.html, last accessed August 19, 2013.
- Shao, G., X. Li, C. Ji. and T. Maeda (2011). Focal mechanism and slip history of 2011 Mw 9.1 off the Pacific coast of Tohoku earthquake, constrained with teleseismic body and surface waves, *Earth Planets Space*, 63 (7), 559-564.
- Shao, G., X. Li, Q. Liu, X. Zhao, T. Yano and C. Ji(UCSB, Maule 2010).Preliminary slip model of the Feb 27, 2010 Mw 8.9 Maule, Chile Earthquake, http://www.geol.ucsb.edu/faculty/ji/big_earthquakes/2010/02/27/chile_2_27.html, last accessed September 24, 2013.
- Sladen A. (Caltech, Tocopilla 2007). Preliminary Result 11/14/2007 (Mw 7.7), Tocopilla Earthquake, Chile. Source Models of Large Earthquakes. http://www.tectonics.caltech.edu/slip_history/2007_tocopilla/tocopilla.html, last

accessed July 1, 2013.

- Sladen A. (Caltech, Maule 2010). Preliminary Result, 02/27/2010 (Mw 8.8), Chile. Source Models of Large Earthquakes. http://www.tectonics.caltech.edu/slip_history/2010_chile/index.html.
- Tanioka, Y., K. Hirata, R. Hino, and T. Kanazawa. (2004). Slip distribution of the 2003 Tokachi-oki earthquake estimated from tsunami waveform inversion. *Earth Planets and Space* 56 (3):373-376.
- Wei S. (Caltech, Sumatra 2012). April/11/2012 (Mw 8.6), Sumatra. Source Models of Large Earthquakes. http://www.tectonics.caltech.edu/slip_history/2012_Sumatra/index.html, last accessed July 1, 2013.
- Wei, S. J., R.W. Graves, D. Helmberger, J.P. Avouac and J.L. Jiang (2012) Sources of shaking and flooding during the Tohoku-Oki earthquake: A mixture of rupture styles, *Earth and Planetary Science Letters*, 333-334, 91-100.
- Wu, C. J., M. Takeo, and S. Ide. (2001). Source process of the Chi-Chi earthquake: A joint inversion of strong motion data and global positioning system data with a multifault model. *Bull. Seis. Soc. Am* 91 (5):1128-1143.
- Yagi, Y. (2004). Source rupture process of the 2003 Tokachi-oki earthquake determined by joint inversion of teleseismic body wave and strong ground motion data, *Earth Planets Space*, 56, 311–316.
- Yagi, Y. and Fukahata, Y., (2011). Rupture process of the 2011 Tohoku-oki earthquake and absolute elastic strain release, *Geophys. Res. Lett.*, 38, L19307, doi:10.1029/2011GL048701.
- Yamanaka, Y., and M. Kikuchi. (2003). Source process of the recurrent Tokachi-oki earthquake on September 26, 2003, inferred from teleseismic body waves. *Earth Planets and Space* 55 (12):E21-E24.
- Yamazaki, Y., T. Lay, K. F. Cheung, H. Yue, and H. Kanamori (2011). Modeling near-field tsunami observations to improve finite-fault slip models for the 11 March 2011 Tohoku earthquake, *Geophys. Res. Lett.*, 38, L00G15, doi:10.1029/2011GL049130.
- Yue, H, T. Lay and K. D. Koper (2012), En Echelon and Orthogonal Fault Ruptures of the 11 April 2012 Great Intraplate Earthquakes. *Nature*, 490, 245-249, doi:10.1038/nature11492.
- Zeng, Y. H., and C. H. Chen. (2001). Fault rupture process of the 20 September 1999 Chi-Chi, Taiwan, earthquake. *Bull. Seis. Soc. Am* 91 (5):1088-1098.
- Zeng, Y., G. Hayes and C. Ji (2007; USGS, Online Model). Preliminary Result of the Nov 14, 2007 Mw 7.7 Antofagasto, Chile Earthquake, http://earthquake.usgs.gov/earthquakes/eqinthenews/2007/us2007jsat/finite_fault

.php, last accessed August 20, 2013.

Zhang, W., T. Iwata, K. Irikura, A. Pitarka, and H. Sekiguchi (2004), Dynamic rupture process of the 1999 Chi-Chi, Taiwan, earthquake, *Geophys. Res. Lett.*, 31, L10605, doi:10.1029/2004GL019827.

Page 3, line 25. For completeness purposes, please provide the scalar seismic moment, M_0 for the corresponding Mw 8.15.

We have done it. [Page 4, line 2]

Page 4. Please clarify or complete the sentence in line 8, because there is a dot at the end of the sentence, so it is not clear what Eq. (4) means or represents. The 2D Fourier spectrum amplitude of what?

We have done it. [Page 4, lines 9-11]

Eq. (4) illustrate that the spectrum of static slip distribution in wavenumber domain is following k^{-2} decay. In Eq. (4), D_{xy} is slip distribution and its spectrum is proportional to k^{-2} . Andrews (1980) derived the k^{-2} from the relationship of slip and stress change.

Page 4. Line 10. Please, to be consistent with the notation in Eq. (4), please clarify the meaning of "F", or, change F by $F_{s,t}$ which represents the 2D discrete Fourier transform of $D_{x,y}$. Also, for completeness purposes, specify that $D_{x,y}$ is the slip distribution over a 2D lattice, for instance.

Thank you. We have done it. [Page 4, line 13]

Page 4. In line 10, please complete, "...wave number.", by "...radial wavenumber."

Thank you. We have done it. [Page 4, line 13]

Page 4. Line 13, please correct "corner frequency" by "corner radial wavenumber", because kc is not a frequency.

Thank you. We have done it. [Page 4, line 16; Page 5, line 7 and Page 15, line 13]

Page 4. Line 14. What happen with the phase beyond kc ? Please, clarify. Or, the last sentence "Within the kc ,...(Geist, 2002)." could be deleted because authors are describing the overall characteristics of the slip and not describing the details of how the random slip is generated numerically in the practice.

We have removed this sentence. Beyond the corner radial wavenumber, kc , the slip spectrum decays with k^{-2} . The generation of random slip is explained in next paragraph, Page 5.

Page 4. Eq. (5). Please, be careful and clear with the mathematical notation. What does F^{-1} represent?. Is it the inverse 2D discrete Fourier transform?

Thank you. We have done it. [Page 4, lines 22-23]

Page 4. Line 23. Please, specify that PDF is Probability Density Function, I think it has not been mentioned before in the text.

Thank you. We have done it. [Page 4, line 27]

PDF is Probability Density Function.

Page 5. Line 3. Complete the units in the sentence, "...5x5 km...", by "...5x5 km²...".

Thank you. We have done it. [Page 5, line 8; Page 5, line 32; Page 16, line 4]

Page 5. Line 3. Please, clarify that 24x14 are along strike and dip respectively.

Thank you. We have done it. [Page 5, line 8]

Page 5. Line 1-4. I will ask the authors to provide some details about how the stochastic slip distribution is generated, and to be clear on the choice of parameters and discuss about the results. Please, read the following comments.

The authors used the values of the Levy PDF suggested by Lavalley et al. (2006), so please clarify in the manuscript that those values were estimated from a stochastic 2D model in the dip slip direction, obtained for the Northridge earthquake. So, why do you use parameters from a shallow crustal earthquake occurred in California to characterize a interplate subduction zone earthquake? Please justify, or discuss.

A: Thank you. We have done it. [Page 5, lines 10-15]

Furthermore, in this study, we do not focus on the values of characteristic for different kinds of faults. Therefore, we decided to simply apply these values which had been published already.

Reference:

Davis, T. L. (1994). 1994 Northridge earthquake. *Nature*, 372, 167.

Notice that according to Lavalley et al (2006) and others, the scaling exponent is $(\nu+1)$ so, the Power Spectrum Density of slip is, $P(k) \sim k^{-(\nu+1)}$, it implies that the slip spectrum behaves as, $D(k) \sim k^{-(\nu+1)/2}$. The authors generate random variables using the Levy distribution, and imposed $P(k) \sim k^{-2}$ as shown in Fig. 1c, so, the slip in the wavenumber domain behaves as, $D(k) \sim k^{-1}$, and Figure 1 is ok, but the slip spectrum does not follow the k^{-2} source characteristic discussed at the beginning of

Section 2.2. Please, clarify this point in the text. Also, discuss the effect in the spatial distribution of slip of this choice (falloff as k^{-1} of the slip spectrum amplitude in the wavenumber domain), versus a slip spectrum that falloff as k^{-2} . From the results shown in Fig. 1, authors generated a slip spectrum that decays as k^{-1} because they imposed the power spectrum density as $P(k) \sim k^{-2}$, but in the legend they say "This slip spectrum decays with exponent of -2 and...", so, it is an inconsistency for me. Please, be clear on the choice, and the terminology used when generating spatial random fields. Herrero & Bernard (1994), Andrews (1981), and others, used a stochastic slip model with a 2D Fourier spectrum that decays as k^{-2} which means, $D(k) \sim k^{-2}$. I am not saying the authors are wrong in their choice, it is only that some parts of the text need some clarification, justification of the choice, or discussion about the assumptions done. We are very sorry for the confusion. In general, the spectrum of slip distribution is proportional to k^{-2} (Herrero and Bernard 1994; Andrews 1980; Tsai 1997). ($|D(k)| \sim k^{-(\nu-1)}$, $\nu=1$) At the beginning of Section 2.2, the Eq. (1) wants to present the spectrum of slip distribution is proportional to k^{-2} . Fig. 1c shows slip spectrum and it consist with k -square. In Lavallee et al (2006), it is formularized by power spectrum density so that there is a disparity of square. We have modified the sentence and Fig. 1c. [Page 4, lines 9-11; Page 15]

Page 5. Line 3. Why did you set a 5x5 subfault size? Did you test different subfault sizes?

For 5x5 km², the resolution of 1 minute (~1.8 km) should be enough to calculate and differentiate the surface deformation.

Page 5. Line 3. Did you assume a constant slip at each subfault? If it is the case, how do you treat the non-smooth slip boundary condition at the boundaries of the fault? Did you apply a taper at all the borders, if not, authors should discuss or justify their treatment?

Page 5. Lines 15-19. Same comment as done in Page 5, line 3, about the assumption of uniform slip at each subfault.

Thank you. We have done it. [Page 5, lines 22-27]

In this study, we do not do any smooth for slip distribution or its boundary. They are complete uniform slip and stochastic process over the fault model. There are two reasons for this application. The first is that we do not have information for where is locked or the location of asperity often repeats in historical event. The second is that there are some studies present the asperity expanding to the boundary of fault model (Ide et al., 2011; Lay et al., 2011; Shao et al., 2011; Yue and Lay 2011). According to these, we do not prefer to apply any extra constraint. If we have more information about

the characteristic of rupture behavior for this region, we would consider giving a constraint.

Reference:

- Ide, S., Baltay, A., and Beroza, G. C. (2011). Shallow dynamic overshoot and energetic deep rupture in the 2011 Mw 9.0 Tohoku-Oki earthquake. *Science*, 332(6036), 1426-1429. doi: 10.1126/science.1207020
- Lay, T., Ammon, C. J., Kanamori, H., Xue, L., and Kim, M. J. (2011). Possible large near-trench slip during the 2011 Mw 9.0 off the Pacific coast of Tohoku Earthquake. *Earth, planets and space*, 63(7), 32. doi:10.5047/eps.2011.05.033
- Shao, G., Li, X., Ji, C., and Maeda, T. (2011). Focal mechanism and slip history of the 2011 Mw 9.1 off the Pacific coast of Tohoku Earthquake, constrained with teleseismic body and surface waves. *Earth, planets and space*, 63(7), 9. doi:10.5047/eps.2011.06.028
- Yue, H., and Lay, T. (2011). Inversion of high-rate (1 sps) GPS data for rupture process of the 11 March 2011 Tohoku earthquake (Mw 9.1). *Geophysical Research Letters*, 38(7). doi: 10.1029/2011GL048700

Page 5, line 15. I would suggest to use "computational domain" instead of "...numerical model".

Thank you. We have done it. [Page 5, line 32]

Page 5. Line 15. Complete the units in $5 \times 5 \text{ km}^2$.

Thank you. We have done it. [Page 5, line 32].

Page 5, lines 21-25. Why do you use 4 min and 1 min for the nested grids? Did you test a different grid size? Which bathymetry/topography is used in the numerical simulation of the tsunami? Please include a reference. For instance, GEBCO (<https://www.gebco.net/>) provides a global 30 arc-sec bathymetry, which has a better resolution than the bathymetry used in this work. Please comment on it. Which is the boundary condition set at the coastlines (the boundary between wet and dry domains)? Do you assume a vertical wall condition, or do you allow inundation? Did you impose any friction, if yes, which one is the Manning's coefficient used in the simulation?

Thank you. We have done it. [Page 6, lines 11-12; Page 6, lines 13-18]

NOAA's open data is used. It is free GEBCO and SRTM. The data can be download from: <https://maps.ngdc.noaa.gov/viewers/wcs-client/>

The Figure 2 presents the time series by uniform slip distribution at station 25 in different resolution of topography. The time series are similar. For resolution, 1 minute

is better than 2 minute and for time spent, 1 minute is less than 30 arc-sec. Therefore, to consider the resolution of simulation and time spent, the resolution of 1 minute was applied. COMCOT is capable of efficiently studying the entire life-span of a tsunami, including its generation, propagation, runup and inundation. COMCOT also supports the nested grid system that the finer grid can be placed on a coarser grid to increase the resolution locally (Wang 2009). In this study, Manning coefficient is 0.013, which represents a smooth surface (Wu, et al., 2008).

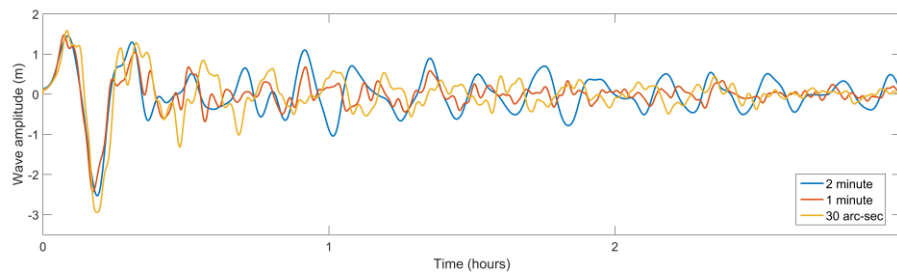


Fig. 2 The time series by uniform slip distribution at station 25 in different resolution of topography. Blue line is 2 minute, red line is 1 minute and yellow line is 30 arc-sec.

Reference:

- Wang, X. (2009). User manual for COMCOT version 1.7 (first draft). Cornell University, 65.
- Wu, T. R., Chen, P. F., Tsai, W. T., and Chen, G. Y.: Numerical Study on Tsunamis Excited by 2006 Pingtung Earthquake Doublet, *Terr. Atmos. Ocean. Sci.*, 19, 705-715, 2008. doi: 10.3319/TAO.2008.19.6.705(PT)

Page 6. Sentence in line 5-6 is a bit confusing, please rephrase to clarify.

We are very sorry for the confusion. We have done it. [Page 6, lines 29-31]

Page 6. Section 3.1. If I understand, authors used the vertical seafloor displacement as initial condition to propagate the tsunami, and the horizontal motion of the seabed is not included in the simulation. I will suggest to clarify better these assumptions in Section 3.1.

We have done it. [Page 6, lines 29-31]

Page 7. Section 3.3. Authors say basically that they computed the probability of the PTA by histograms, but from my understanding they show (Fig. 5) a probability density estimated from the numerical PTA data. I think authors could say/argue a little bit more about this, in terms of this choice and analysis. I mean, does the data follow any

distribution (e.g. Gaussian, Levy, Log-normal)? Are the PTA data (simulated) Gaussian distributed? Is it possible to estimate the probability of exceeding a certain input value from these numerical results? I think some of these aspect is not discussed or mentioned in the text.

We have added in the text. [Page 8, lines 11-13]

Page 7. Line 11. Please complete the idea that after generating the second set of slip models, the tsunami is simulated.

We have done it. [Page 8, lines 2-6]

The histograms, first set, and black lines, second set, are similar. The second set illustrate that the PTA distribution by 100 times tsunami simulations is approximately reliable.

Page 7. Paragraph 3. When you compare PTA versus distance, how do you define or measure the distance between source and station? At least, it could be mentioned or discussed in the text.

We have done it. [Page 8, line 22]

Page 8. Lines 14-16. Please, provide the references for the Maule, Tohoku and Sumatra earthquakes.

We have done it. [Page 9, line 6-8]

Reference:

Chile earthquake (Lay et al., 2010; Fritz et al., 2011)

Lay, T., Ammon, C. J., Kanamori, H., Koper, K. D., Sufri, O., & Hutko, A. R. (2010). Teleseismic inversion for rupture process of the 27 February 2010 Chile (Mw 8.8) earthquake. *Geophysical Research Letters*, 37(13).

Fritz, H. M., Petroff, C. M., Catalan, P. A., Cienfuegos, R., Winckler, P., Kalligeris, N., Weiss, R., Barrientos, S. E., Meneses, G., Valderas-Bermejo, C., Ebeling, C., Papadopoulos, A., Contreras, M., Almar, R., Dominguez, J. C., and Synolakis, C. E. (2011). Field survey of the 27 February 2010 Chile tsunami. *Pure and Applied Geophysics*, 168(11), 1989-2010.

Tohoku earthquake (Goda et al., 2015; Goda and Song, 2016)

Goda, K., and Song, J. (2016). Uncertainty modeling and visualization for tsunami hazard and risk mapping: a case study for the 2011 Tohoku earthquake. *Stochastic Environmental Research and Risk Assessment*, 30(8), 2271-2285.

Goda, K., Yasuda, T., Mori, N., and Mai, P. M. (2015). Variability of tsunami inundation

footprints considering stochastic scenarios based on a single rupture model: application to the 2011 Tohoku earthquake. *Journal of Geophysical Research: Oceans*, 120(6), 4552-4575.

Sumatra earthquake (Lay et al., 2005)

Lay, T., Kanamori, H., Ammon, C. J., Nettles, M., Ward, S. N., Aster, R. C., ... & DeShon, H. R. (2005). The great Sumatra-Andaman earthquake of 26 December 2004. *Science*, 308(5725), 1127-1133.

Page 8. Lines 22-31. The results discussed here are obtained at several sites, but It is not clear where the sites (tides gauges) are exactly located, right at the boundary, or surrounded by a wet domain even during the tsunami evolution? If the latter is true, the comparison of maximum tsunami wave height (this study) is not exactly straightforward comparable to runup (analyzed in other studies). Also, authors should comment on the effect (or limitations) of the grid resolution (1 arc-min, used in this study) over the results obtained. I suspect this coarse grid may have an effect on the simulations near the coast.

Thank you. These stations are surrounded by a wet domain so that we have modified this part. [Page 9, lines 13-22]

In comment of **Page 5, lines 21-25**, we provide a test in different resolution of topography to prove that the resolution of 1 minute can be accepted.

Page 8, line 17. Clarify what "lecture" means.

We have done it. [Page 9, line 9]

Page 9. Line 29. I would suggest to complete the idea in the sentence, "Furthermore, interpolation has a tremendous effect for the exponent value becoming larger with grid size reducing (Tsai, 1997).", because it refers to how the exponent and correlation lengths are computed from the solutions of slip models of earthquakes. On the other hand, some authors assume k-2 slip models based on other physical considerations.

We have done it. [Page 10, lines 18-20]

Interpolation for a given geometry will affect the exponent of k. For example, the exponent value of the original slip model of the Northridge earthquake from Zeng and Anderson (1996) is 1.876 in Tsai (1997). The slip model is interpolated by making the dimension of the element size one-half of the original size (0.5x0.5 km²). The slip distribution is smoothed by the interpolation and the new exponent value is 3.767. The exponent value is 4.202 when the slip model is interpolated by making the dimension of the element size one-fourth of the original size. Our point from mathematical

operation is that interpolation make original pattern smoother as a filter depresses the short wavenumber and enhancing the long wavenumber.

===== Figures =====

Figure 1. Clarify units, X? k? length km or 5km? To avoid misunderstanding, I suggest to delete the label "Northridge earthquake" in the Fig 1a, and you can mention it in the caption (e.g. Levy parameters were taken from Lavallee et al.....obtained for the Northridge earthquake.), because the realization shown is for an Mw 8.15 earthquake and not for the Northridge earthquake. Fault axis along dip and strike are confusing too. I will suggest to plot the real distance along strike and dip directions (with the correct units) and not the "indexes" of each subfault. What do represent the colorbar? See my comments about P(k) and D(k), what is shown in Fig 1c is not what is written in the caption.

We have done it. [Page 15]

X is random variable (the filtered slip) so that the unit of X is meter. The unit of k is $\text{km}^{-1} ((k_x^2+k_y^2)^{-2})$.

Figure 2. I suggest to contextualize at the beginning the region of the study area, (e.g. Map of Taiwan...for example). Correct 5x5 km by 5x5 km^2 . Is the white box the nested inner grid? Colorbar?

We have done it. [Page 16]

The colorbar presents the elevation in km.

Figure 3. I would suggest specify that the "energy propagation" corresponds to, maximum tsunami wave height, for instance. Colorbar?

We have done it. [Page 17, lines 1-2]

The colorbar presents the maximum tsunami wave height in meter (b, d, and f).

===== Tables =====

Table 1. The description of the table and caption is a bit confusing. What is the meaning of Max(uni)? A suggestion is that a part of the description given at the end of the table can be moved to the caption, and authors can put the units [m] directly beneath each variable description.

We have modified it. [Pages 20-21]

Max(uni) means the maximum wave height in uniform slip case.

Assessment of peak tsunami amplitude associated with a great earthquake occurring along the southernmost Ryukyu subduction zone for Taiwan region

Yu-Sheng Sun¹, Po-Fei Chen¹, Chien-Chih Chen¹, Ya-Ting Lee¹, Kuo-Fong Ma¹ and Tso-Ren Wu²

5 ¹Department of Earth Sciences, National Central University, Taoyuan City, Taiwan 320, R.O.C.

²Graduate Institute of Hydrological and Oceanic Sciences, National Central University, Taoyuan City, Taiwan 320, R.O.C.

Correspondence to: Yu-Sheng Sun (shengfantasy@gmail.com)

Abstract. The southernmost portion of the Ryukyu Trench closed to Taiwan island is a potential region to generate 7.5 to 8.7 tsunami earthquakes by shallow rupture. The fault model for this potential region dips 10° northward with rupture length of 10 120 km and width of 70 km. The earthquake magnitude estimated by fault geometry is Mw 8.15 with 8.25 m average slip as a constrain of earthquake scenario. The heterogeneous slip distributions over rupture surface are generated by stochastic slip model, the slipspectrum with k^{-2} decay in wave number domain, and they are consistent with above identical seismic conditions. The results from tsunami simulation illustrate that the propagation of tsunami waves and the peak wave heights largely vary in response to the slip distribution. The wave phase changing is possible as the waves propagate, even under the same seismic 15 conditions. The tsunami energy path is not only following the bathymetry but also depending on slip distribution. The probabilistic distributions of peak tsunami amplitude calculated by 100 different slip patterns from 30 recording stations reveal the uncertainty decreases with distance from tsunami source. The highest wave amplitude for 30 recording points is 7.32 m at Hualien for 100 different slips. Comparing with stochastic slips, uniform slip distribution will be extremely underestimated, especially in near field. In general, uniform slip assumption only represents the average phenomenon so that it will ignore 20 possibility of tsunami wave. These results indicate that considering effect of heterogeneous slip distribution is necessary for assessing tsunami hazard and that can provide more information about tsunami uncertainty for a more comprehensive estimation.

1 Introduction

Almost all destructive tsunamis are generated by shallow earthquakes that occur at subduction zone. There were recently 25 destructive tsunami events: the 2004, Mw 9.1, Sumatra earthquake (Lay et al., 2005), the 2010, Mw 8.8, Chile earthquake (Lay et al., 2010; Fritz et al., 2011) and the 2011, Mw 9.0, Tohoku earthquake (Goda et al., 2015; Goda and Song, 2016); all of them occurred at subduction zone. The island of Taiwan located at the convergent boundary between the Philippine Sea Plate and the Eurasian Plate is possibly threatened from tsunami. The convergence rate in this area is approximately 80-85 mm/yr (Seno et al., 1993; Yu et al., 1997; Sella et al., 2002; Hsu et al., 2009; Hsu et al., 2012). Thus, earthquakes occur frequently in

and around Taiwan. The shallow earthquakes that occur in the Manila Trench to the south and the Ryukyu Trench to the northeast are particularly tsunamigenic. Also, the earthquakes in southernmost Ryukyu Trench is more active than north Manila Trench (Wu et al., 2013). The most well-known historic tsunami events that have occurred in northeast Taiwan are the 1867 Keelung earthquake (M_w 7.0) (Tsai 1985; Ma and Lee, 1997; Cheng et al., 2016; Yu et al., 2016) and the 1771 Yaeyama (Japan) earthquake (M_w ~8) (Nakamura, 2009a). The historic recording demonstrates that Taiwan island has the potential of tsunami threat. Furthermore, the 2011 Tohoku earthquake induced powerful tsunami that destroyed coastal areas and caused nuclear accidents (Mimura et al., 2011). There are four nuclear power plants along the coast on Taiwan island so that it is necessary to carefully estimate the tsunami hazard and compound disasters.

Probabilistic tsunami hazard analysis (PTHA) is a modification of probabilistic seismic hazard analysis (PSHA) (Cornell, 1968; SSHAC, 1997), and it is intended to forecast as comprehensively as possible the probability of tsunami hazards for a given region. Considering tsunamis triggered by earthquakes, the recurrence rates of earthquakes have typically been estimated using the Gutenberg–Richter relationship (Gutenberg and Richter, 1944) for a defined source region. The assessment of wave heights is one of the primary differences between PTHA and PSHA. PSHA assesses ground motion based on empirical attenuation relationships (Wang et al., 2016). PTHA assesses tsunami wave heights using empirical approaches or tsunami simulations (Geist, 2002; Geist and Parsons, 2006; Geist and Parsons, 2009). Geist and Parsons (2006) mentions that the tsunami wave height follows a definable frequency-size distribution over a sufficiently long amount of time at a given coastal region (Soloviev, 1969; Houston et al., 1977; Horikawa and Shuto, 1983; Burroughs and Tebbens, 2005). This method is of great use in establishing tsunami probability for regions if there is an extensive catalog of observed tsunami wave heights. Given the wide distribution of global tsunamigenic earthquakes within seafloor regions at subduction zones, the tsunami records obtained from coastal gauges or/and ocean buoys are too sparse to assess the associated hazards comprehensively, and the recording time since their deployment is too short to enable study of the recurrence intervals of tsunamis/earthquakes. The existing tsunami catalogue is limited so that the simulation is an effective approach. Conventional tsunami simulation adopts simple source approximation and applies elastic dislocation theory to calculate the deformation of the seafloor surface assuming a uniform slip over entire fault surface (Okada, 1985; Okal, 1982). However, the complexity of earthquake ruptures plays a substantial role in tsunami generation. Conventional approaches are therefore unable to capture various features of short-wavelength tsunamis in the near field (Geist, 2002; Geist and Parsons, 2009). Previous studies that simulate tsunamis resulting from historical earthquakes around Taiwan (Ma and Lee, 1997; Wu et al., 2008) using uniform slip models agree only with long-wavelength observations. For hazard mitigation, it is critical that the amplitudes of tsunamis are predicted along various coasts for a given earthquake as accurately as possible. To make such predictions, the effects of rupture complexity must be taken into consideration. Recent developments in PTHA have included the adoption of stochastic slip distributions of earthquakes to determine the overall probability of particular tsunami heights. (Geist and Parsons, 2006, 2009). That method can be able to quantify the variations for a reasonable estimation in evaluating the probability of specified tsunami heights at individual locations that result from a specific fault.

In this study, we assess tsunami heights along the coasts of Taiwan that is caused by the potential tsunamigenic zone at the southernmost end of the Ryukyu subduction zone. This potential zone is close to Taiwan and at least ten earthquakes ($M_w > 7$) have occurred over the past 100 years (Hsu et al., 2012). The largest one is M_w 7.7 in 1920 (Theunissen et al., 2010). For this area, the plausible magnitude of greatest earthquake was determined to a range between 7.5 and 8.7 (M_w) (Hsu et al., 2012). The fault zone is bounded by the Longitudinal Valley Fault to the west and the Gagua Ridge to the east (Hsu et al., 2012). This defined fault geometry with rupture length and width was employed and earthquake with magnitude 8.15 is used in the tsunami simulations. The stochastic slip model is invoked to describe the uncertainty of the rupture pattern over the fault plane to enable a more realistic assessment of tsunami probability.

10 2 Great earthquake scenario and tsunami simulation

2.1 Assessment of Seismic Parameters

The estimating magnitude of the maximum possible earthquake scenario is essential for the fundamental seismic condition of tsunami simulation. This scenario, potential rupture fault, proposed by Hsu et al. (2012) occurs along the southernmost Ryukyu trench with rupture length of 120 km, width of 70 km and dip of 10° and extends to a depth of 13 km. Kanamori and Anderson (1975) investigated the relation between rupture area and moment, which revealed that the most average stress drops ($\Delta\sigma$) between 10 to 100 bars. The average stress drops for the most interplate earthquakes are around 30 bars so that we set an average stress drop of 30 bars. According to the stress drop and seismic moment (M_0) relations in dip slip faults (Kanamori and Anderson, 1975):

$$20 \quad M_0 = \frac{\pi(\lambda+2\mu)}{4(\lambda+\mu)} \Delta\sigma W^2 L \quad (1)$$

W and L is width and length of rupture plane respectively. We can obtain the moment for this scenario under the average stress drop of 30 bars and with a definite rupture geometry. In Eq. (1), μ is rigidity and λ is the Lamè parameter. We assume that the crust is elastic and homogeneous. Hence, $\mu = \lambda = 30$ GPa (Fowler, 2004; Piombo et al, 2007). Additionally, the seismic moment can be presented by rupture area and average slip as below (Lay and Wallace, 1995):

$$25 \quad M_0 = \mu A \bar{D} \quad (2)$$

The seismic moment, moreover, is dependent on rupture area (A) and average slip (\bar{D}) so that the average slip can be estimated by following Eq. (2) and it is 8.25 m. Then the seismic moment can be transformed magnitude M_w by (Hanks and Kanamori, 1979)

$$M_w = \left(\frac{\log M_0}{1.5} \right) - 10.73 \quad (3)$$

Therefore, the maximum possible earthquake is M_w 8.15 ($M_0 = 2.07 \times 10^{28}$).

2.2 Stochastic Slip Model

- 5 The rupture process of an earthquake is extremely complex. The seismic inversion results reveal the slip distribution of rupture is heterogeneous with temporal development. Using a simplified uniform slip distribution to simulate tsunami only captures the long-wavelength portion of the tsunami fields (Geist and Dmowska, 1999). In addition, the temporal description of the seismic rupture process can be ignored because the propagation velocity of the tsunami waves is substantially slower than the seismic rupture velocity (Dean and Dalrymple, 1991; Ma et al., 1991; Wang and Liu, 2006). Andrews (1980) showed that
- 10 static slip distribution is directly related to stress changes and the spectrum of slip distribution is proportional to k^{-2} decay in wavenumber domain:

$$|F_{s,t}[D_{x,y}]| \propto k^{-2} \quad (4)$$

- $D_{x,y}$ is the slip distribution over a 2D lattice, $F_{s,t}$ is the 2D Fourier transform, $k = \sqrt{k_x^2 + k_y^2}$ is the radial wavenumber. k^{-2} power law illustrates slip distribution has self-similar characteristics and from the fractal perspective, this characteristic also can be demonstrated (Tsai, 1997). Herrero and Bernard (1994) based on self-similar introducing the k -square model which leads to the ω -square model (Aki, 1967). The slip spectrum follows k^{-2} decay beyond the corner radial wavenumber, k_c , which is proportional to $1/L_c$. The L_c depends on characteristic rupture dimension (Geist, 2002).
- 15

- The heterogeneous slip distribution is proportional to k^{-2} and is similar to a fractional Brownian motion as a stochastic process (Tsai, 1997). The stochastic slip distribution can be described by convolution in Fourier domain,
- 20

$$D_{x,y} \propto F_{x,y}^{-1}[F_{s,t}[X_{x,y}] \times k^{-2}] \quad (5)$$

- where $X_{x,y}$ is random variable for spatial distribution; moreover, it makes phase random. $F_{x,y}^{-1}$ is the inverse 2D Fourier transform. The random distribution, X , which is best described by a non-Gaussian distribution, especially by a Lèvy distribution, can be calculated by reversing Eq. (5) (Lavallée and Archuleta 2003; Lavallée et al., 2006). Lèvy distribution can be described
- 25 by 4 parameters α , β , γ and μ_L . as below:

$$\varphi(t) = \begin{cases} \exp\left(-\gamma^\alpha |t|^\alpha \left[1 + i\beta \operatorname{sign}(t) \tan \frac{\pi\alpha}{2} (|\gamma t|^{1-\alpha} - 1)\right] + i\mu_L t\right), & \alpha \neq 1 \\ \exp\left(-\gamma |t| \left[1 + i\beta \frac{2}{\pi} \operatorname{sign}(t) (\ln|t| + \ln\gamma)\right] + i\mu_L t\right) & , \alpha = 1 \end{cases} \quad (6)$$

The parameter α , $0 < \alpha \leq 2$, affects the falloff rate of probability density function (PDF) for the tail. The parameter β , $-1 \leq \beta \leq 1$, controls the skewness of PDF. The parameter γ , $\gamma > 0$, controls the width of PDF. The parameter μ_L , $-\infty < \mu_L < \infty$, is related to the

location of PDF. Lèvy distribution is good to describe the distribution of random variable, X , from real earthquake events, which implies the slip distribution without self-similar characteristic has heavy tail behavior (Lavallée et al., 2006). From the experiments of generating stochastic slip distribution, the heavy tail behavior affects the intensity of extreme value (Lavallée and Archuleta 2003).

5

The stochastic slip distribution is generated by 2D spatial random distribution with convoluting self-similar characteristic beyond the **corner radial wavenumber**, constraining by rupture dimension, in wavenumber domain. In this study, the potential rupture fault is divided into $5 \times 5 \text{ km}^2$ subfaults. **The number of grid mesh is 24×14 which are along strike and dip respectively.** The spatial random variable produced adopts Lèvy distribution ($\alpha=1.51, \beta=0.2, \gamma=28.3, \mu_L=-0.9$) which is the dip slip result from Lavallée et al (2006) as Figure 1a. **In Lavallée et al. (2006), the slip distribution of Northridge earthquake had been divided into the dip slip and strike slip directions and calculated by inverse 2D stochastic model to obtain the values of the Lèvy PDF. The values of the Lèvy PDF are given over to dip slip. The Northridge earthquake is a thrust earthquake (Davis 1994) so that it roughly has similar mechanism with our scenario fault model. In addition, the inversed slip distribution in study region is lack to do the analysis of Lèvy PDF. Therefore, the value of Lèvy distribution in Lavallée et al. (2006) is adopted in this study.** In the perspective of mathematical operation, the slip distribution in Eq. (5) is a kind of filtered random distribution. However, for consistency with the physical behavior over the rupture surface supposed by the results of inverse method, the truncation has to be applied to the Lèvy distribution to constrain the extreme slip value. The synthetic slip distribution (Fig. 1b) produced by spatial random distribution in Figure 1a is heterogeneous and its power spectrum obeys k -square model at high wavenumber (Fig. 1c). The average slip of this synthetic slip distribution is 8.25 m, which represents earthquake energy keeping a constant as estimating above, and maximum slip is 31.02 m. The 100 different slip distributions are produced for tsunami simulation. They represent the uncertainty of results of complex rupture process. In 100 sets, the maximum slip range is between 20.17 to 37.97 m. **There are no smooth process and extraregional constrain for slip distribution. There are two reasons for this application. The first is that we do not have information for where is locked or the location of asperity often repeats in historical event. The second is that there are some studies present the asperity expanding to the boundary of fault model (Ide et al., 2011; Lay et al., 2011; Shao et al., 2011; Yue and Lay, 2011). According to these, we do not prefer to apply any extra constraint for stochastic slip distributions. By same token, the uniform slip case is a complete uniform slip distribution.** Figure 1b and 1d are the stochastic distribution of the scenario source models causing the maximum and minimum wave height at the recording station 26 (Hualien) (Fig. 2). Both patterns affecting the propagation will show at Sect. 3.1.

30

2.3 Numerical Tsunami Simulation

Figure 2 shows **computational domain**, recording stations and fault model. The potential rupture fault is divided into $5 \times 5 \text{ km}^2$ subfaults, and the stochastic slip distribution model is applied to determine the amount of discrete slip on each subfault. Vertical

seafloor displacements caused by rupture slip are calculated using elastic dislocation theory (Okada, 1985). The Cornell Multigrid Coupled Tsunami Model (COMCOT) is used to perform the tsunami simulations. COMCOT is capable of efficiently studying the entire life-span of a tsunami, including its generation, propagation, runup and inundation (Wang 2009). It has been widely used in studying many historical tsunami events, such as 1960 Chilean tsunami (Liu et al., 1995), 1992 Flores Islands tsunami (Liu et al., 1995), 2003 Algeria tsunami (Wang and Liu, 2005), 2004 Indian Ocean tsunami (Wang and Liu, 2006, 2007), and 2006 Ping-Tung tsunami, Taiwan (Wu, et al., 2008; Chen, et al., 2008). COMCOT solves the linear or nonlinear shallow water equations for spherical or Cartesian coordinates using the finite difference method. With the flexible nested grid system, it can properly exhibit both efficiency and accuracy from the near-coastal region to the far-field region. Two grid layers are used to simulate the propagation of tsunamis. The Manning coefficient is 0.013 in this study to assume a sandy sea bottom (Wu, et al., 2008). The bathymetry adopted NOAA's (National Oceanic and Atmospheric Administration) open data which can be download from <https://maps.ngdc.noaa.gov/viewers/wcs-client/> (Amante and Eakins, 2009). The resolution of the outer layer is 4 minutes for the solution of the linear shallow water equation, and the resolution of the inner layer is 1 minute for the solution of the nonlinear form of the shallow water equation. There are 30 recording stations which refer to the positions of tidal gauges maintained by the Central Weather Bureau (CWB) along the coasts of Taiwan and the outlying islands. The website of CWB presents the location of tide stations <http://e-service.cwb.gov.tw/HistoryDataQuery/index.jsp> and http://www.cwb.gov.tw/V7e/climate/marine_stat/tide.htm. These locations are shifted slightly to the node of grid in order to record accurately. Table 1 presents the locations of recording stations.

20 **3 The effect of heterogeneous slip on the tsunamis**

The stochastic slip model produces different slip distributions with the same fault geometry, average slip and a constant seismic moment. The model is used to describe the heterogeneous slip pattern of earthquake and to further examine its effect on the tsunamis occurring at the southernmost end of the Ryukyu subduction zone adjacent to Taiwan. According to the previous sections, the maximum possible earthquake is determined to be M_w 8.15 with 8.25 m average slip. Furthermore, the uniform slip distribution on the rupture plane is also used to simulate tsunami for discussing the different between uniform and heterogeneous slip on the tsunamis.

3.1 Initial water elevation and energy propagation

The static vertical displacement of the ocean floor is modelled using the elastic dislocation theory (Okada, 1985) and considered static slip distribution. The vertical seafloor displacement is used to be initial water level, and the horizontal component of the seabed is not included in the simulation. Figure 3a shows the initial water elevations produced by uniform

slip distribution and Figure 3b is its maximum free-surface elevation during the propagation. Figure 3c and 3e are the initial water elevations produced by stochastic slip distributions (Fig. 1b and 1d). The initial water elevation by uniform slip is simple and smooth, but for the stochastic slip models are more complex and more heterogeneous. Nonuniform slip causes an apparent change in the wavelength distribution of the initial free-surface elevation (the potential energy distribution), which affects the path of energy propagation. In the uniform slip scenario, the maximum free-surface elevation pattern is clear and controlled by topography. However, many strong and seemingly chaotic paths of wave energy appear in the nonuniform scenarios, and the ocean surface field has more uncertainties in terms of flow. In Figure 3b, the maximum free-surface elevation mainly travels toward two places where the seafloor elevation becomes shallower, relative to the deep areas northeast of Taiwan as bathymetry in Fig. 2. Although the propagation by nonuniform slip distributions (Fig. 3d and 3f) also has the same characteristics, it is notable that the paths followed by the wave energy differ, which depends on the rupture pattern. At the northeast of Taiwan in Figure 3f, there is a strong wave path connecting the two higher elevation part. However, this behavior does not occur in Figure 3b and 3d. Besides that, at the footwall side, the maximum elevation of Figure 3d is higher than Figure 3f. In Figure 3b, the high elevation only appears along the coast at footwall side. These results indicate the wave energy variation depends on rupture pattern causing differences in wave paths and leads to totally different tsunami amplitudes.

15

3.2 Wave characteristic

There are 30 stations along the coasts for recording the motion of sea level. Relative to other stations, the station 25 (Shihti), 26 (Hualien) and 27 (Suao) are near the potential rupture fault, and they have high wave amplitude and enormous variation in the tsunami simulation of 100 different slip distributions so that the time series of wave heights at these stations are shown as an example (Fig. 4). The varied wavelength distribution of the initial free-surface elevation results in substantial phase changes and different wave heights. It's worth noting that the average of the disordered and chaotic time series produced by the 100 different slip distributions is almost identical to the results from the uniform case. This implies the uniform case simply represents an average result and it cannot represent all of the possible situations.

25 According to the statistical results from 100 different slip patterns (Table 1) for 30 stations, Hualien station has the maximum wave amplitude, 7.32 m, and its maximum wave amplitude interval is 1.87 to 7.32 m. It is the widest interval for any recording site and the standard deviation of this distribution is 1.024. These indicate that Hualien station has high uncertainty in this scenario setting. However, the maximum wave amplitudes from uniform slip are relatively lower than stochastic results. Following above lecture, we need to rethink about that the estimation of uniform slip case is available for hazard analysis or not, even only focusing on the maximum wave amplitude issue.

30

3.3 The peak tsunami amplitude probability

According to the results of our simulations, we calculated the probability of the peak/maximum tsunami amplitudes (PTA) at each recording station as shown in Figure 5 by histogram. To verify the representativeness of the PTA probability distributions, another 100 sets of different slip distributions had been produced with same seismic conditions and simulated. In Figure 5, the shapes of PTA distributions from another 100 sets, black lines, are similar to the histograms, the first 100 sets. This results verify the representativeness of the PTA probability distributions in 100 sets. This test also reinforces the reproducibility of our simulations and demonstrates that the number of simulations is roughly satisfactory for statistical analysis. Of course, the more slip distribution we use, the more comprehensive and stable the range we obtain.

- 10 In Figure 5, the PTA distributions at eastern Taiwan, red markers, are obviously higher than the western, blue markers, due to the specified location of the source of tsunami. The shapes of PTA distributions at eastern Taiwan seem like log-normal distribution and at western, they seem like normal distribution. We suppose that the attenuation of wave propagation causes the shape of log-normal distribution degenerating into normal distribution. The PTA produced by uniform slip are generally located in the middle of the PTA distributions. Both of the PTA values from uniform slip distribution and the values of the
- 15 PTA from stochastic slip distribution models decrease with the distance from potential fault because of the attenuation of wave propagation (Fig. 5 is for all stations and Fig. 6 shows station 20 to 30 in the eastern Taiwan). However, some stations are not perfectly following this, for instance, station 17, 19 and 21 which could be affected by coastal topography and energy channel. From Figure 3d, station 21 comparing with neighbor coast is exactly at the location where the energy gathers. In addition, the broad distributions frequently occur at promontories along the coastline and are caused by complex propagation path effects
- 20 between the source region and the recording locations (Geist, 2002). There are many compound factors to affect the tsunami propagation and maximum wave height. Figure 6 presents the relation between distance and wave height and also shows the PTA distribution as Figure 5. The distance is the shortest between the stations and fault plane. On the footwall side, the station 20 and 22 are outer island. They do not face the energy path directly (Fig. 3f) so that the PTA distributions are lower than station 21 and 23; even though the distance from fault are similar. On the hanging wall, station 29 is far from coast comparing
- 25 other stations because of real location of station and numerical grid setting so that the PTA distribution is lower than station 30 (Fig. 3b). The PTA distributions and their average values roughly appear a linear decrease with distance except the near field, station 26 and 27. Moreover, the ranges of PTA distributions convergent with distance, too. On the other hand, the near field, station 26 and 27, are directly affected by seafloor deformation so that the PTA by uniform slip are quite low.
- 30 Although the seismic parameters have defined already in our experiment and been held constants, there exist an uncertainty for PTA rather than a constant value. The uniform case cannot provide it and the PTA could be underestimated. Results give specific PTA ranges, which are the wave height uncertainties for the scenario of the earthquakes from Ryukyu Trench. It is necessary to consider the effect by heterogeneous slip distribution for a comprehensively assessing tsunami hazard.

4 Discussion

4.1 Tsunami

5 Most coast threatened by near-field tsunami is parallel the subduction zone like the coast of Chile, Japan and Indonesia. There are many tsunami event occurring these regions such as the 2010, Mw 8.8, Chile earthquake (Lay et al., 2010; Fritz et al., 2011), the 2011, Mw 9.0, Tohoku earthquake (Goda et al., 2015; Goda and Song, 2016), the 2004, Mw 9.1, Sumatra earthquake (Lay et al., 2005), and the 2010, Mw 8.1, Mentawai earthquake (Satake et al., 2013). However, the potential rupture fault in this study along the southernmost Ryukyu subduction zone is perpendicular to the coast of Taiwan island, which directly affects the first movement of wave. On the footwall, the first movement is up, but conversely, it is down. On the hanging wall, the coastline backs from land to sea at first tsunami wave that help people have more time to leave seafont.

The effect by heterogeneous slip is important and necessary to consider for the near field estimation (Geist, 2002 and Ruiz et al., 2015). Figure 5 shows that the PTA distributions in the near field are broad and narrow with distance increasing from potential fault. The uncertainty in near field is higher than far field. At the most of east stations, the values of average PTA approach uniform results, but at station 25 and 26, their uniform slip results are close to minimum PTA (Table 1.). Geist (2002) presents average and extrema PTA in nearshore calculated for 100 different slip distributions and compares with uniform slip result (Figure 6a in Geist, (2002)). The range of PTA also narrows with distance increasing. The values of uniform slip result and average of PTA are similar, but there are some average values close to minimum PTA around 19°N to 19.5°N. There is similar characteristic of average PTA and uniform results in different region. The average PTA is equal to uniform slip result in nearshore, but that could be caused by the factors (e.g. distance to the tsunami source, propagation path, etc.) to affect the average PTA to close to minimum PTA.

There are four nuclear power plants (NPP) on the Taiwan island. According to the numerical results, we infer that the PTA mean value of NPP4 coastal area is around 2 to 3 m. This distribution may be wilder than other nuclear power plants due to the relative position of tsunami source. Moreover, NPP4 locates a bay with curved shape so that the extra magnification effect perhaps makes PTA higher. The NPP3 also has this condition and then the energy concentrates at this area (Fig 3b, 3d and 3f). For NPP1 and NPP2 coastal area, the PTA distributions are between 1 and 2 m. The coast of this two nuclear power plants is facing the tsunami current slightly so that its PTA should be higher than neighbor coast (Fig 3b, 3d and 3f). In general, under this scenario, the coast of NPP4 has largest threat. Although the NPP3 is far from this tsunami source, it roughly faces 1.5 m wave height on average and has ± 0.5 m uncertain range. However, the NPP3 is more close to Manila subduction zone which

could be threatened by the tsunami from Manila Trench. The coast of NPP1 and NPP2 is relative safe and has less uncertainty for PTA.

5 The use of a heterogeneous slip pattern clearly delineates the range of possible waveforms and provides more information on latent uncertainties of wave height. The 95% confidence intervals for wave height from 100 sets present in each time series and provide us a specific range for the motion of sea level (Fig. 4). According to these time series, we are aware of the periods of tsunami runup and runoff and can prepare the supporting policies to reduce disaster. For example, a nuclear power plant has the trench of water intake from ocean for cooling reactor, and if the motion of sea level is too low to take the water, the temperature of reactor will be too high and then cause the nuclear disaster. This issue is necessary to pay attention in Taiwan
10 because there are four unclear power plants located near the coast.

4.2 Stochastic slip model

The results of tsunami simulations illustrate that the effect of the slip distribution on the rupture plane has a significant effect on wave propagation and wave height. The correctness of this slip distribution determines whether the wave height calculations
15 represent a useful reference or not. However, some parameters of stochastic model could influence synthetic slip distributions. For instance, the exponent of slip spectrum associates with roughness of slip distribution. Higher exponential value inhibits the power of high wavenumber and leads it smoother; conversely, lower value leads it rougher. In general, k -square model needs to be followed. **Furthermore, interpolation of slip distribution for a given geometry will affect the exponent of k (Tsai, 1997). Interpolation make original pattern smoother. The short wavenumber will be depressing and the long wavenumber will
20 be enhancing.** Additionally, the random spatial variability of the slip distribution is more critical. According to Lavallée and Archuleta (2003) and Lavallée et al., (2006), we adopted the truncated non-Gaussian distribution as a spatial variability. Truncation limits the non-Gaussian distribution to a particular range. The extreme truncation will cause the heavy-tailed characteristic of this distribution to become less pronounced or even disappear, as in a Gaussian distribution. The synthetic slip is a filtering process in mathematics so that the heavy-tailed characteristic affects the extremum of slip distribution. The
25 maximum slip will be greater as the truncated range increases. The maximum slip may exceed reasonable values as truncated range is too wide. Therefore, the parameters must be chosen carefully in order to match the observations acquired by inversion.

5 Conclusion

The maximum possible earthquake scenario is M_w 8.15 with average slip of 8.25 m in the southernmost portion of the Ryukyu
30 Trench. The 100 slip distributions of the seismic rupture surface were generated by a stochastic slip model. The maximum slip range is between 20.17 to 37.97 m and the average slip all consists with 8.25 m. The heterogeneous slip induces variability in

tsunami wave heights and the associated paths of propagation. The simulated results demonstrate that rupture complexity has a significant influence on the near field for local tsunamis. The PTA distribution provide a specific range for wave height and its occurring probability in this scenario. These distributions and their average values roughly appear a linear decrease with distance. The coast, which is very close tsunami source or even upon, is directly affected by rupture slip. Then, the range of PTA distribution will converge with distance increasing from tsunami source. In this study, Hualien station, which is upon the source, has the wildest PTA interval (1.87-7.32 m) and the highest wave amplitude. The statistical summary reveals this station, whose standard deviation is 1.63 and larger than other stations, has the largest uncertainty. However, the PTA caused by the uniform slip distribution is only 1.63 m, which is much lower, even below average (3.36 m) in this station. It implies that a simplified earthquake source cannot completely represent tsunami amplitudes in reality. If we adopt uniform slip to assess tsunami hazard, it will be critically underestimated. The tsunami amplitudes, which have characteristically extreme variance, are imperative for assessing tsunami hazards and the quantitative techniques is also important.

References

- Aki, K.: Scaling law of seismic spectrum, *J. Geophys. Res.*, 72, 1217-1231, 1967. doi:10.1029/JZ072i004p01217
- 15 Amante, C. and Eakins, B. W.: ETOPO1 1 arc-minute global relief model: procedures, data sources and analysis, US Department of Commerce, National Oceanic and Atmospheric Administration, National Environmental Satellite, Data, and Information Service, National Geophysical Data Center, Marine Geology and Geophysics Division Colorado, 2009. doi:10.7289/V5C8276M
- Andrews, D. J.: A stochastic fault model: 1. Static case, *J. Geophys. Res. Solid Earth*, 85, 3867-3877, 1980. doi:10.1029/JB085iB07p03867
- 20 Burroughs, S. M. and Tebbens, S. F.: Power-law scaling and probabilistic forecasting of tsunami runup heights, *Pure Appl. Geophys.*, 162, 331-342, 2005. doi:10.1007/s00024-004-2603-5
- Chen, P.-F., Newman, A. V., Wu, T.-R., and Lin, C.-C.: Earthquake Probabilities and Energy Characteristics of Seismicity Offshore Southwest Taiwan, *Terr. Atmos. Ocean. Sci.*, 19, 2008. doi:10.3319/TAO.2008.19.6.697(PT)
- 25 Cheng, S.-N., Shaw, C.-F., and Yeh, Y. T.: Reconstructing the 1867 Keelung Earthquake and Tsunami Based on Historical Documents, *Terr. Atmos. Ocean. Sci.*, 27, 2016. doi:10.3319/TAO.2016.03.18.01(TEM)
- Cornell, C. A.: Engineering seismic risk analysis, *Bull. Seism. Soc. Am.*, 58, 1583-1606, 1968.
- Davis, T. L. and Namson, J. S.: A Balanced Cross-Section of the 1994 Northridge Earthquake, Southern California, *Nature*, 372, 167-169, 1994. doi:10.1038/372167a0
- 30 Dean, R. G. and Dalrymple, R. A.: *Water wave mechanics for engineers and scientists*, World Scientific Publishing Co Inc, 1991. doi:10.1142/9789812385512_0004

- Fowler, C. M. R.: *The Solid Earth: An Introduction to Global Geophysics*, Cambridge University Press, Cambridge. pp. 728. 2004. ISBN-10: 0521893070
- Fritz, H. M., Petroff, C. M., Catalán, P. A., Cienfuegos, R., Winckler, P., Kalligeris, N., Weiss, R., Barrientos, S. E., Meneses, G., Valderas-Bermejo, C., Ebeling, C., Papadopoulos, A., Contreras, M., Almar, R., Dominguez, J. C., and Synolakis, C. E.:
 5 Field Survey of the 27 February 2010 Chile Tsunami, *Pure Appl. Geophys.*, 168, 1989-2010, 2011. doi:10.1007/s00024-011-0283-5
- Geist, E. L.: Complex earthquake rupture and local tsunamis, *J. Geophys. Res. Solid Earth*, 107, ESE 2-1-ESE 2-15, 2002. doi:10.1029/2000JB000139
- Geist, E. L. and Dmowska, R.: Local Tsunamis and Distributed Slip at the Source. In: *Seismogenic and Tsunamigenic
 10 Processes in Shallow Subduction Zones*, Sauber, J. and Dmowska, R. (Eds.), Birkhäuser Basel, Basel, 1999. doi:10.1007/978-3-0348-8679-6_6
- Geist, E. L. and Parsons, T.: Probabilistic Analysis of Tsunami Hazards*, *Nat. Hazards*, 37, 277-314, 2006. doi:10.1007/s11069-005-4646-z
- Geist, E. L. and Parsons, T.: Assessment of source probabilities for potential tsunamis affecting the U.S. Atlantic coast, *Mar.
 15 Geol.*, 264, 98-108, 2009. doi:10.1016/j.margeo.2008.08.005
- Goda, K. and Song, J.: Uncertainty modeling and visualization for tsunami hazard and risk mapping: a case study for the 2011 Tohoku earthquake, *Stoch Environ Res Risk Assess*, 30, 2271-2285, 2016. doi:10.1007/s00477-015-1146-x
- Goda, K., Yasuda, T., Mori, N., and Mai, P. M.: Variability of tsunami inundation footprints considering stochastic scenarios based on a single rupture model: Application to the 2011 Tohoku earthquake, *J. Geophys. Res. Oceans*, 120, 4552-4575, 2015.
 20 doi:10.1002/2014JC010626
- Gutenberg, B. and Richter, C. F.: Frequency of earthquakes in California, *Bull. Seism. Soc. Am.*, 34, 185-188, 1944.
- Hanks, T. C. and Kanamori, H.: A moment magnitude scale, *J. Geophys. Res. Solid Earth*, 84, 2348-2350, 1979. doi:10.1029/JB084iB05p02348
- Herrero, A. and Bernard, P.: A Kinematic Self-Similar Rupture Process for Earthquakes, *Bull. Seism. Soc. Am.*, 84, 1216-
 25 1228, 1994.
- Horikawa, K. and Shuto, N.: *Tsunami disasters and protection measures in Japan*, *Tsunamis-Their Science and Engineering*, Terra Scientific Publishing Company, 1983. 9-22, 1983.
- Houston, J. R., Carver, R. D., and Markle, D. G.: *Tsunami-Wave Elevation Frequency of Occurrence for the Hawaiian Islands*, Army Engineer Waterways Experiment Station, Vicksburg, MS, 66 pp, 1977.
- 30 Hsu, Y.-J., Ando, M., Yu, S.-B., and Simons, M.: The potential for a great earthquake along the southernmost Ryukyu subduction zone, *Geophys. Res. Lett.*, 39, n/a-n/a, 2012. doi:10.1029/2012GL052764
- Hsu, Y.-J., Yu, S.-B., Simons, M., Kuo, L.-C., and Chen, H.-Y.: Interseismic crustal deformation in the Taiwan plate boundary zone revealed by GPS observations, seismicity, and earthquake focal mechanisms, *Tectonophysics*, 479, 4-18, 2009. doi:10.1016/j.tecto.2008.11.016

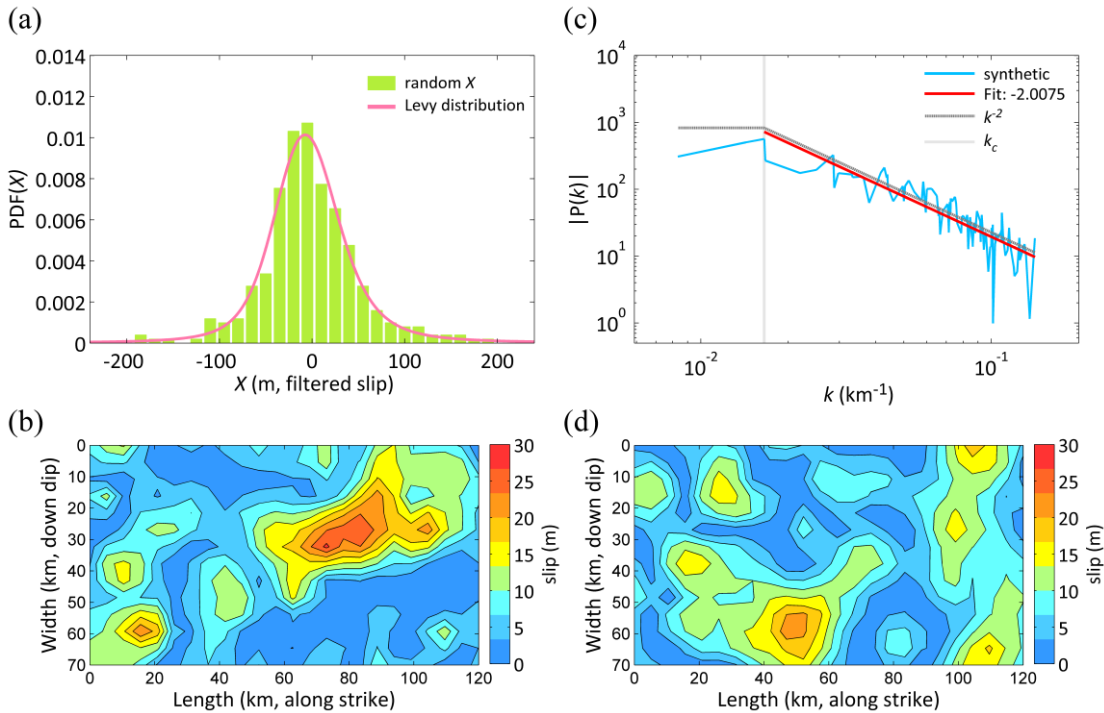
- Ide, S., Baltay, A., and Beroza, G. C.: Shallow dynamic overshoot and energetic deep rupture in the 2011 Mw 9.0 Tohoku-Oki earthquake, *Science*, 332, 1426-1429, 2011. doi:10.1126/science.1207020
- Kanamori, H. and Anderson, D. L.: Theoretical basis of some empirical relations in seismology, *Bull. Seism. Soc. Am.*, 65, 1073-1095, 1975.
- 5 Lavallée, D. and Archuleta, R. J.: Stochastic modeling of slip spatial complexities for the 1979 Imperial Valley, California, earthquake, *Geophys. Res. Lett.*, 30, 1245, 2003. doi:10.1029/2002GL015839
- Lavallée, D., Liu, P., and Archuleta, R. J.: Stochastic model of heterogeneity in earthquake slip spatial distributions, *Geophys. J. Int.*, 165, 622-640, 2006. doi:10.1111/j.1365-246X.2006.02943.x
- Lay, T., Ammon, C. J., Kanamori, H., Koper, K. D., Sufri, O., and Hutko, A. R.: Teleseismic inversion for rupture process of the 27 February 2010 Chile (Mw 8.8) earthquake, *Geophys. Res. Lett.*, 37, L13301, 2010. doi:10.1029/2010GL043379
- 10 Lay, T., Ammon, C. J., Kanamori, H., Xue, L., and Kim, M. J.: Possible large near-trench slip during the 2011 Mw 9.0 off the Pacific coast of Tohoku Earthquake, *Earth Planets Space*, 63, 32, 2011. doi:10.5047/eps.2011.05.033
- Lay, T., Kanamori, H., Ammon, C. J., Nettles, M., Ward, S. N., Aster, R. C., Beck, S. L., Bilek, S. L., Brudzinski, M. R., Butler, R., DeShon, H. R., Ekström, G., Satake, K., and Sipkin, S.: The Great Sumatra-Andaman Earthquake of 26 December 15 2004, *Science*, 308, 1127-1133, 2005. doi:10.1126/science.1112250
- Lay, T. and Wallace, T. C.: *Modern global seismology*, Academic press, 1995. ISBN: 9780127328706
- Liu, P. L. F., Cho, Y. S., Yoon, S. B., and Seo, S. N.: Numerical Simulations of the 1960 Chilean Tsunami Propagation and Inundation at Hilo, Hawaii. In: *Tsunami: Progress in Prediction, Disaster Prevention and Warning*, Tsuchiya, Y. and Shuto, N. (Eds.), Springer Netherlands, Dordrecht, 1995. doi:10.1007/978-94-015-8565-1_7
- 20 Liu, P. L. F., Cho, Y. S., Briggs, M. J., Kanoglu, U., and Synolakis, C. E.: Runup of solitary waves on a circular Island, *J. Fluid Mech.*, 302, 259-285, 1995. doi:10.1017/S0022112095004095
- Ma, K.-F. and Lee, M.-F.: Simulation of historical tsunamis in the Taiwan region, *Terr. Atmos. Ocean. Sci.*, 8, 13-30, 1997.
- Ma, K.-F., Satake, K., and Kanamori, H.: The origin of the tsunami excited by the 1989 Loma Prieta Earthquake —Faulting or slumping?, *Geophys. Res. Lett.*, 18, 637-640, 1991. doi:10.1029/91GL00818
- 25 Mimura, N., Yasuhara, K., Kawagoe, S., Yokoki, H., and Kazama, S.: Damage from the Great East Japan Earthquake and Tsunami - A quick report, *Mitig Adapt Strat Gl*, 16, 803-818, 2011. doi:10.1007/s11027-011-9297-7
- Nakamura, M.: Fault model of the 1771 Yaeyama earthquake along the Ryukyu Trench estimated from the devastating tsunami, *Geophys. Res. Lett.*, 36, n/a-n/a, 2009. doi:10.1029/2009GL039730
- Okada, Y.: Surface deformation due to shear and tensile faults in a half-space, *Bull. Seism. Soc. Am.*, 75, 1135-1154, 1985.
- 30 Okal, E. A.: Mode-wave equivalence and other asymptotic problems in tsunami theory, *Phys. Earth Planet. Inter.*, 30, 1-11, 1982. doi:10.1016/0031-9201(82)90123-6
- Piombo, A., Tallarico, A., and Dragoni, M.: Displacement, strain and stress fields due to shear and tensile dislocations in a viscoelastic half-space, *Geophys. J. Int.*, 170, 1399-1417, 2007. doi:10.1111/j.1365-246X.2007.03283.x

- Ruiz, J. A., Fuentes, M., Riquelme, S., Campos, J., and Cisternas, A.: Numerical simulation of tsunami runup in northern Chile based on non-uniform $k-2$ slip distributions, *Nat. Hazards*, 79, 1177-1198, 2015. doi:10.1007/s11069-015-1901-9
- Satake, K., Nishimura, Y., Putra, P. S., Gusman, A. R., Sunendar, H., Fujii, Y., Tanioka, Y., Latief, H., and Yulianto, E.: Tsunami Source of the 2010 Mentawai, Indonesia Earthquake Inferred from Tsunami Field Survey and Waveform Modeling, *Pure Appl. Geophys.*, 170, 1567-1582, 2013. doi:10.1007/s00024-012-0536-y
- 5 Sella, G. F., Dixon, T. H., and Mao, A.: REVEL: A model for Recent plate velocities from space geodesy, *J. Geophys. Res. Solid Earth*, 107, ETG 11-11-ETG 11-30, 2002. doi:10.1029/2000JB000033
- Senior Seismic Hazard Analysis Committee (SSHAC): Recommendations for probabilistic seismic hazard analysis: guidance on uncertainty and use of experts, US Nuclear Regulatory Commission Washington, DC, 1997. doi:10.2172/479072
- 10 Seno, T., Stein, S., and Gripp, A. E.: A model for the motion of the Philippine Sea Plate consistent with NUVEL-1 and geological data, *J. Geophys. Res. Solid Earth*, 98, 17941-17948, 1993. doi:10.1029/93JB00782
- Shao, G., Li, X., Ji, C., and Maeda, T.: Focal mechanism and slip history of the 2011 Mw9.1 off the Pacific coast of Tohoku Earthquake, constrained with teleseismic body and surface waves, *Earth Planets Space*, 63, 9, 2011. doi:10.5047/eps.2011.06.028
- 15 Soloviev, S.: Recurrence of tsunamis in the Pacific, *Tsunamis in the Pacific Ocean*, 1970. 149-163, 1970.
- Theunissen, T., Font, Y., Lallemand, S., and Liang, W.-T.: The largest instrumentally recorded earthquake in Taiwan: revised location and magnitude, and tectonic significance of the 1920 event, *Geophys. J. Int.*, 183, 1119-1133, 2010. doi:10.1111/j.1365-246X.2010.04813.x
- Tsai, C.-C. P.: Slip, Stress Drop and Ground Motion of Earthquakes: A View from the Perspective of Fractional Brownian Motion, *Pure Appl. Geophys.*, 149, 689-706, 1997. doi:10.1007/s000240050047
- 20 Tsai, Y.-B.: A study of disastrous earthquakes in Taiwan, 1683–1895, *Bull. Inst. Earth Sci., Acad. Sin.* 5, 1-44, 1985
- Wang, X.: User manual for COMCOT version 1.7 (first draft). Cornell University, 65., 2009.
- Wang, X. M. and Liu, P. L. F.: A numerical investigation of Boumerdes-Zemmouri (Algeria) earthquake and tsunami, *CMES Comput. Model. Eng. Sci.*, 10, 171-183, 2005. doi:10.3970/cmes.2005.010.171
- 25 Wang, X. and Liu, P. L. F.: An analysis of 2004 Sumatra earthquake fault plane mechanisms and Indian Ocean tsunami, *J. Hydraul. Res.*, 44, 147-154, 2006. doi:10.1080/00221686.2006.9521671
- Wang, X. and Liu, P. L. F.: Numerical simulations of the 2004 Indian Ocean tsunamis — coastal effects, *J. Earthquake and Tsunami*, 01, 273-297, 2007. doi:10.1142/s179343110700016x
- Wang, Y.-J., Chan, C.-H., Lee, Y.-T., Ma, K.-F., Shyu, J., Rau, R.-J., and Cheng, C.-T.: Probabilistic seismic hazard assessment for Taiwan, *Terr. Atmos. Ocean. Sci.*, 27, 2016. doi:10.3319/TAO.2016.05.03.01(TEM)
- 30 Wu, T.-R., Chen, P.-F., Tsai, W.-T., and Chen, G.-Y.: Numerical Study on Tsunamis Excited by 2006 Pingtung Earthquake Doublet, *Terr. Atmos. Ocean. Sci.*, 19, 705-715, 2008. doi:10.3319/TAO.2008.19.6.705(PT)
- Wu, Y.-H., Chen, C.-C., Turcotte, D. L., and Rundle, J. B.: Quantifying the seismicity on Taiwan, *Geophys. J. Int.*, 194, 465-469, 2013. doi:10.1093/gji/ggt101

Yu, N.-T., Yen, J.-Y., Chen, W.-S., Yen, I. C., and Liu, J.-H.: Geological records of western Pacific tsunamis in northern Taiwan: AD 1867 and earlier event deposits, *Mar. Geol.*, 372, 1-16, 2016. doi:10.1016/j.margeo.2015.11.010

Yu, S.-B., Chen, H.-Y., and Kuo, L.-C.: Velocity field of GPS stations in the Taiwan area, *Tectonophysics*, 274, 41-59, 1997. doi:10.1016/S0040-1951(96)00297-1

- 5 Yue, H. and Lay, T.: Inversion of high-rate (1 sps) GPS data for rupture process of the 11 March 2011 Tohoku earthquake (Mw 9.1), *Geophys. Res. Lett.*, 38, L00G09, 2011. doi:10.1029/2011GL048700



- 10 **Fig. 1. (a) The spatial random variable: truncated Lévy distribution. Lévy parameters obtained from the Northridge earthquake were taken from Lavallée et al (2006). (b) A stochastic slip is generated from filtering the spatial random variable \bar{X} , Fig. 1a. This slip pattern produces the highest maximum wave amplitude at Hualien station. (c) Slip spectrum is calculated from Fig. 1b. This slip spectrum decays with exponent of -2 and characteristic of corner radial wavenumber r . It verifies that synthetic slip is identical with k -square model and condition of rupture dimension. (d) This stochastic slip distribution produces the lowest maximum wave amplitude at Hualien station.**
- 15

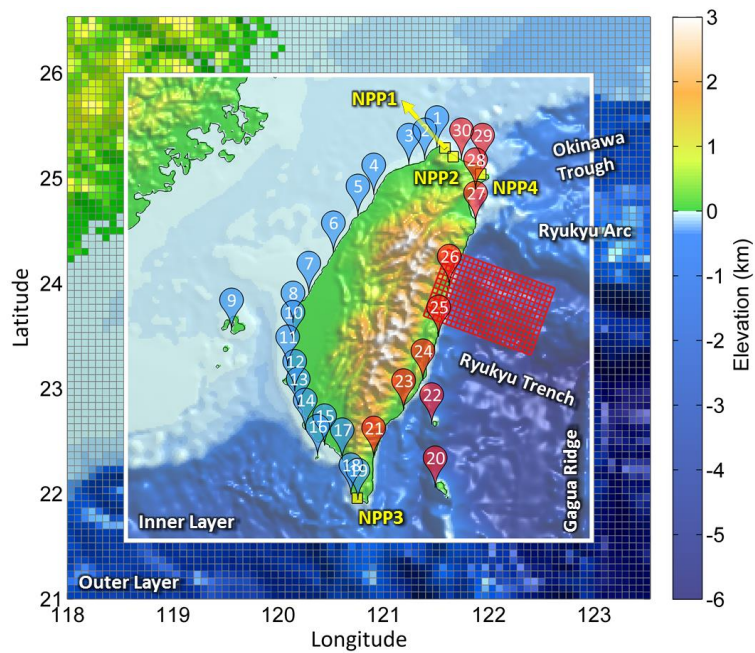


Fig. 2. The map of Taiwan presents the fault model and recoding stations used in this study. The bathymetry is divided into 2 layer for different resolutions. The resolution of the outer layer is 4 minutes, and the resolution of the inner layer of the white box is 1 minute. The red grid denotes the potential fault model (5×5 km²). Pins represent 30 tidal gauges of the CWB. The red and blue colors indicate stations on the east and west sides of Taiwan respectively. Yellow squares represent the sites of the nuclear power plants.

5

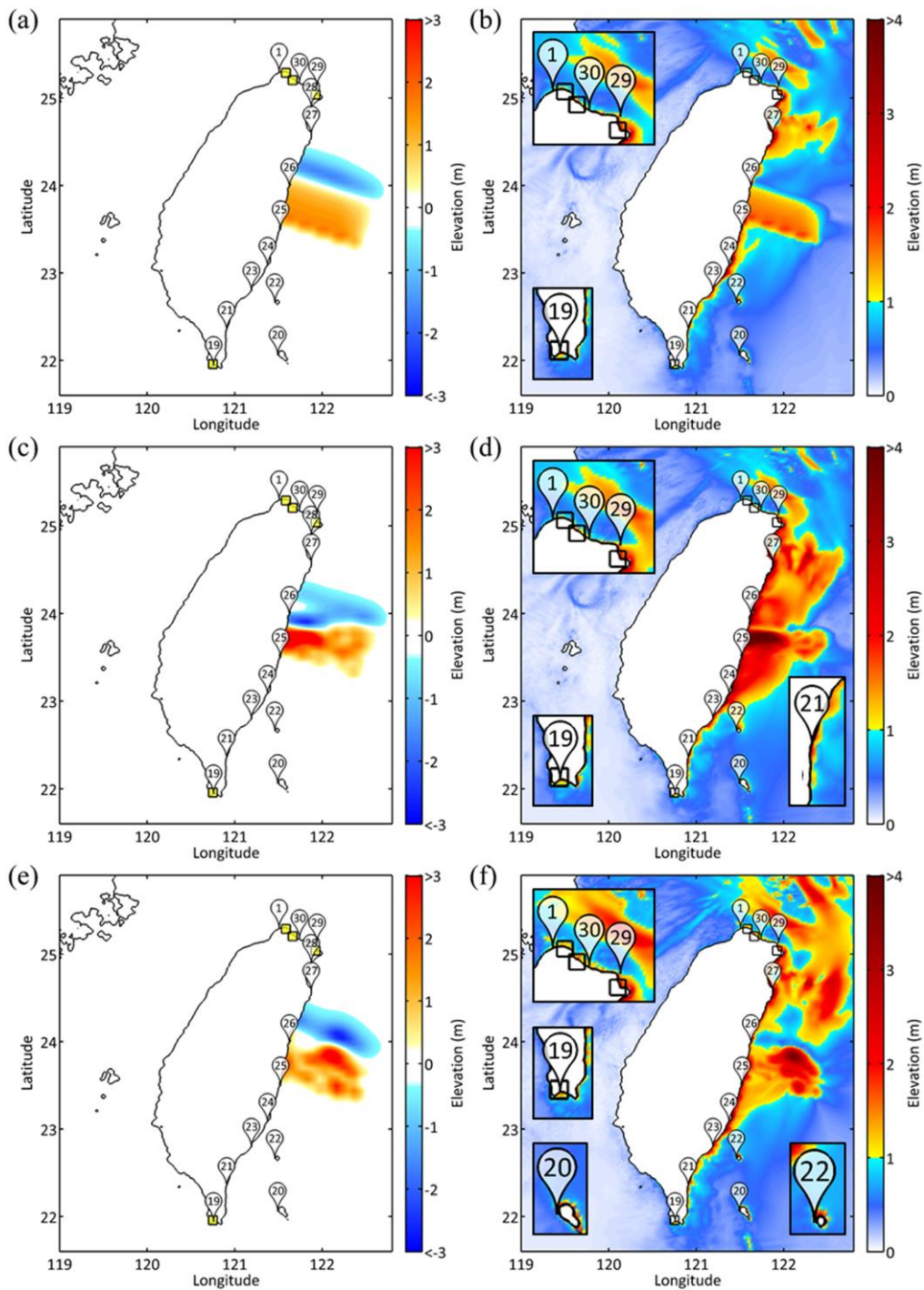
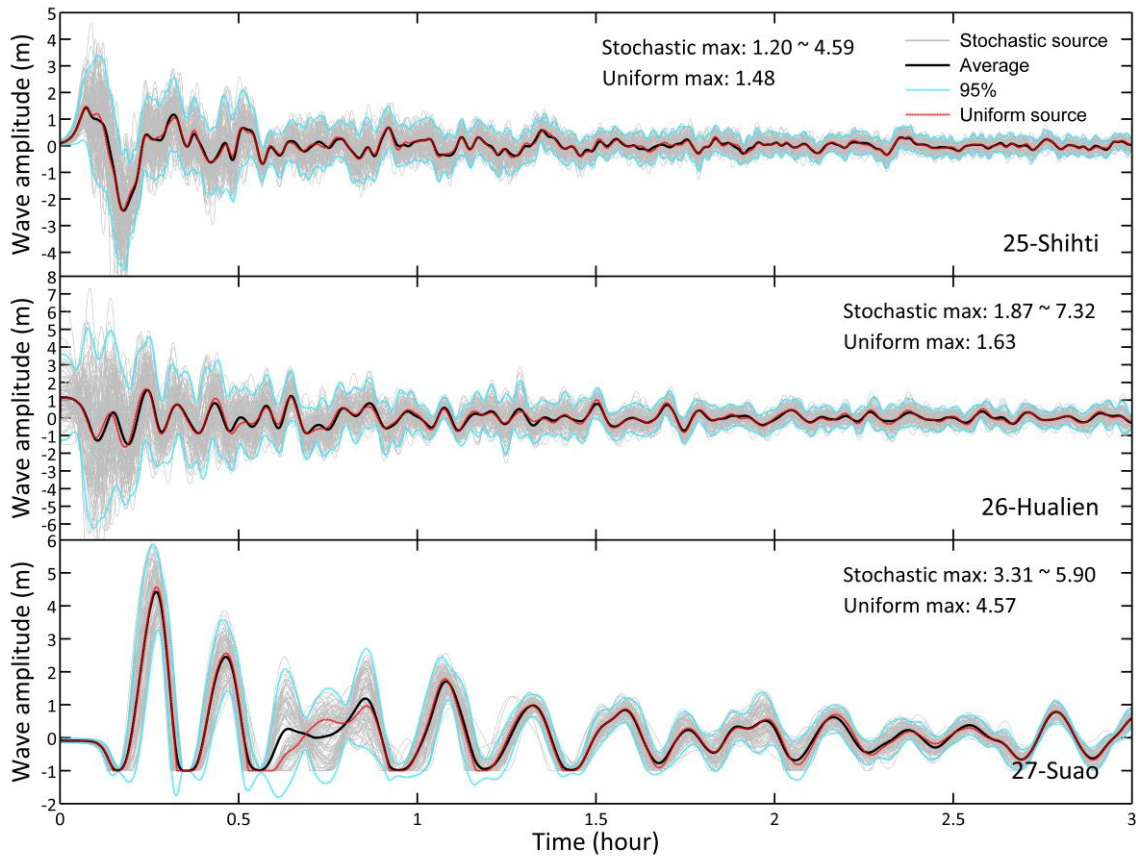


Fig. 3. (a), (c) and (e) are the initial water elevation and colorbar represents the elevation of initial water surface. (b), (d) and (f) are maximum free-surface elevation, the distribution of energy path, and colorbar represents the elevation of maximum free-surface. (a) and (b) displays the results from uniform slip distribution. (c) and (d) displays the results from Fig. 1b. (e) and (f) displays the results

from Fig. 1d. In fundamental, seafloor dominants tsunami propagation, but the slip distribution has strong influence. In (a, c and e), yellow squares represent nuclear power plants; in (b, d and f), they are open squares.



5 Fig. 4. The time series of wave heights recorded at station 25 (Shihti), 26 (Hualien) and 27 (Suao). Gray lines represent the time series of 100 different slip distributions; black lines represent the averages of the gray lines; blue lines represent the 95% confidence intervals; and red lines are the time series produced using uniform slip distributions. Parts of the wave heights on station 27 are lower than water depths, and these curves have been truncated.

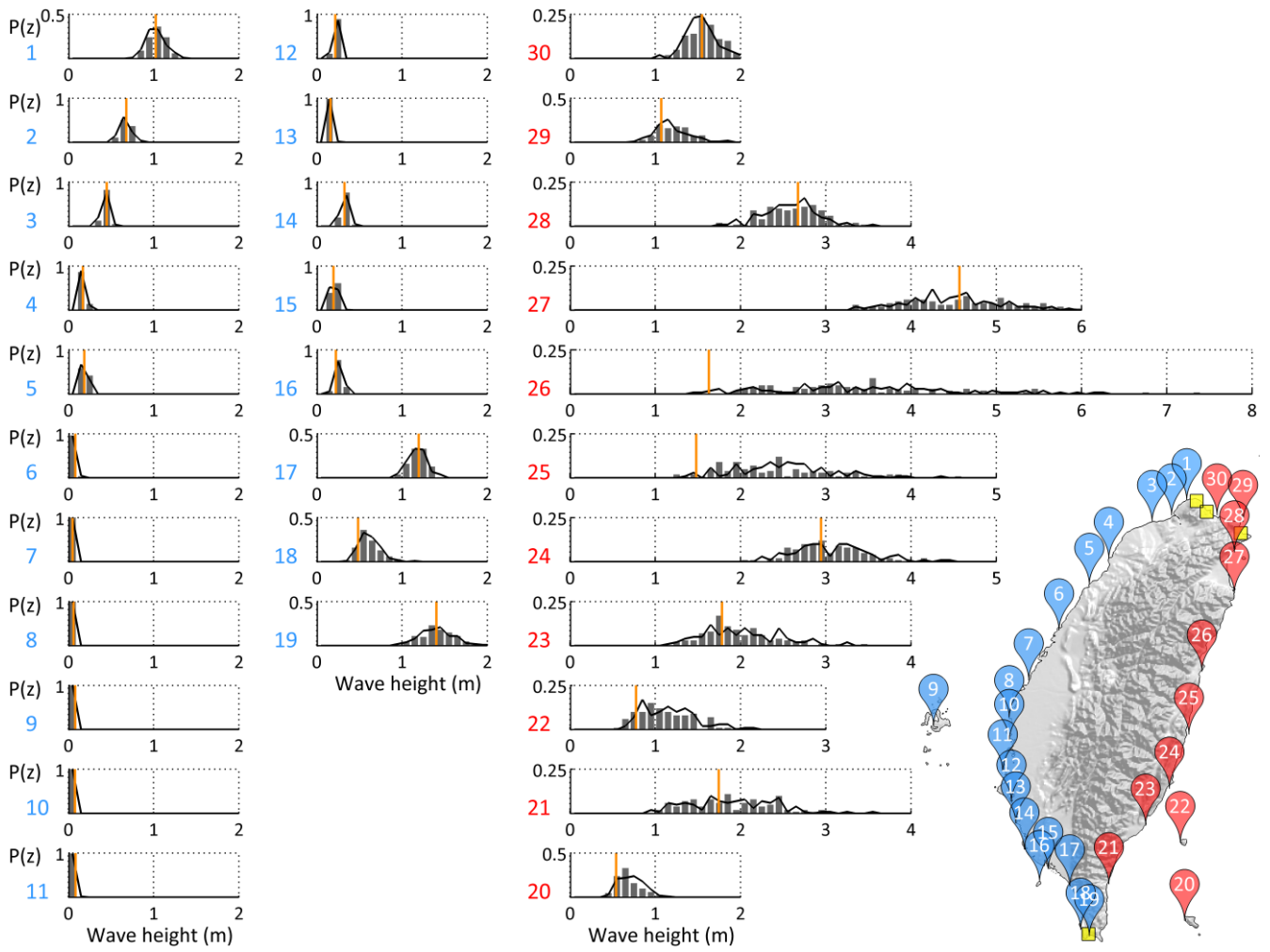
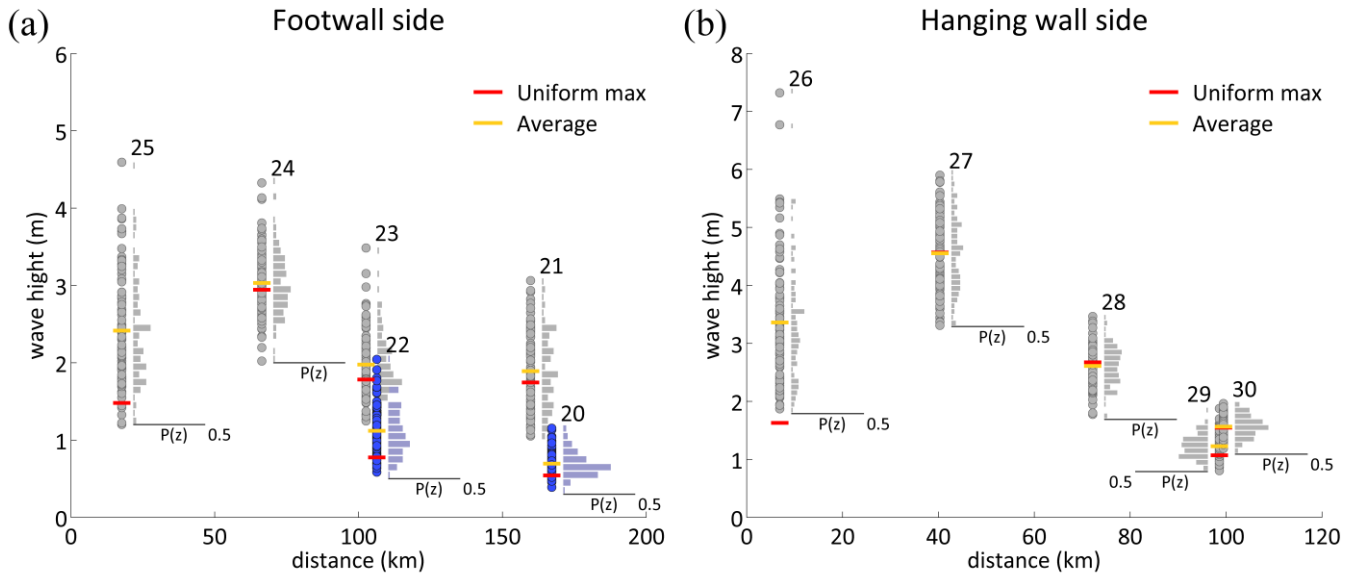


Fig. 5. The probabilities of PTA along the coast of Taiwan (blue: 1~19, red: 20~30). The histograms display the PTA derived from 100 different slip simulations. The black lines represent the results from another 100 simulations, and the orange lines represent the PTA obtained using a uniform slip distribution. The PTA probability distribution give a clear PTA range and its occurring probability.

5



5 **Fig. 6.** The relation between distance and wave height for stations from 20 to 30 in the eastern Taiwan. (a) is the station on the footwall side. Station 20 and 22, blue color, are out of Taiwan island. (b) is the stations on the hanging wall side. Both sides roughly appear a linear decay and uncertainty range converging with distance increasing for tsunami amplitude. Red bars show the PTA of the uniform slip distribution and yellow bars show the average of the PTA from stochastic slip models.

Table 1. This table lists the maximum, minimum, standard deviation and average wave heights for the PTA probability distributions in meter. It also lists the maximum wave heights from uniform slip model.

#	Station	Lon.	Lat.	Min [m]	Max [m]	σ [m]	Avg. [m]	Max [m] (uniform slip)
1	Linshanbi	121.5106	25.2844	0.80	1.32	0.108	1.04	1.02
2	Danshuei	121.4019	25.1844	0.55	0.83	0.061	0.68	0.68
3	Jhuwei	121.2353	25.1200	0.33	0.52	0.039	0.44	0.45
4	Hsinchu	120.9122	24.8503	0.13	0.24	0.025	0.17	0.17
5	Waipu	120.7717	24.6514	0.15	0.26	0.020	0.20	0.19
6	Taichung Port	120.5250	24.2917	0.07	0.11	0.009	0.08	0.08
7	Fanyuan	120.2972	23.9147	0.04	0.06	0.004	0.05	0.05
8	Bozihliao	120.1417	23.6250	0.05	0.07	0.004	0.06	0.06
9	Penghu	119.5669	23.5636	0.07	0.09	0.005	0.08	0.08
10	Dongshih	120.1417	23.4417	0.06	0.09	0.005	0.08	0.08
11	Jiangjyun	120.1000	23.2181	0.06	0.10	0.007	0.09	0.09

12	Anping	120.1583	22.9750	0.15	0.26	0.018	0.22	0.22
13	Yongan	120.1917	22.8083	0.11	0.20	0.016	0.16	0.16
14	Kaohsiung	120.2883	22.6144	0.23	0.43	0.039	0.33	0.33
15	Donggang	120.4417	22.4583	0.15	0.28	0.026	0.21	0.20
16	Siaoliuciou	120.3750	22.3583	0.17	0.40	0.046	0.26	0.22
17	Jiahe	120.6083	22.3250	0.90	1.44	0.098	1.19	1.20
18	Syunguangzuei	120.6917	21.9917	0.33	0.96	0.124	0.61	0.49
19	Houbihu	120.7583	21.9417	0.90	1.96	0.197	1.41	1.40
20	Lanyu	121.4917	22.0583	0.39	1.15	0.155	0.69	0.54
21	Dawu	120.8972	22.3375	1.05	3.06	0.487	1.89	1.74
22	Lyudao	121.4647	22.6622	0.58	2.04	0.316	1.12	0.78
23	Fugang	121.1917	22.7917	1.25	3.48	0.409	1.98	1.78
24	Chenggong	121.3767	23.0889	2.02	4.33	0.416	3.03	2.94
25	Shihti	121.5250	23.4917	1.20	4.59	0.680	2.42	1.48
26	Hualien	121.6231	23.9803	1.87	7.32	1.024	3.36	1.63
27	Suao	121.8686	24.5856	3.31	5.90	0.641	4.55	4.57
28	Gengfang	121.8619	24.9072	1.78	3.47	0.337	2.61	2.67
29	Longdong	121.9417	25.1250	0.80	1.88	0.202	1.23	1.07
30	Keelung	121.7417	25.1750	1.19	1.96	0.183	1.57	1.55
